The Plant Cell, Vol. 28: 2097–2116, September 2016, www.plantcell.org

MYB107 and MYB9 Homologs Regulate Suberin Deposition in Angiosperms

Justin Lashbrooke,[a,b,c] Hagai Cohen,[a] Dorit Levy-Samocha,[a] Oren Tzfadia,[a,1] Irina Panizel,[a] Viktoria Zeisler,[d] Hassan Massalha,[a] Adi Stern,[a] Livio Trainotti,[e] Lukas Schreiber,[d] Fabrizio Costa,[b] and Asaph Aharoni[a,2]

[a] Department of Plant and Environmental Sciences, Weizmann Institute of Science, Rehovot 76100, Israel
[b] Research and Innovation Centre, Foundation Edmund Mach, I-38010 San Michele all'Adige, Trento, Italy
[c] ARC Infruitec-Nietvoorbij, Stellenbosch 7599, South Africa
[d] Department of Ecophysiology, IZMB, University of Bonn, 53115 Bonn, Germany
[e] Department of Biology, University of Padova, 35121 Padova, Italy

ORCID IDs: 0000-0003-4511-4215 (J.L.); 0000-0002-8829-8205 (L.T.); 0000-0001-7003-9929 (L.S.); 0000-0003-1416-1078 (F.C.)

Suberin, a polymer composed of both aliphatic and aromatic domains, is deposited as a rough matrix upon plant surface damage and during normal growth in the root endodermis, bark, specialized organs (e.g., potato [*Solanum tuberosum*] tubers), and seed coats. To identify genes associated with the developmental control of suberin deposition, we investigated the chemical composition and transcriptomes of suberized tomato (*Solanum lycopersicum*) and russet apple (*Malus x domestica*) fruit surfaces. Consequently, a gene expression signature for suberin polymer assembly was revealed that is highly conserved in angiosperms. Seed permeability assays of knockout mutants corresponding to signature genes revealed regulatory proteins (i.e., AtMYB9 and AtMYB107) required for suberin assembly in the *Arabidopsis thaliana* seed coat. Seeds of *myb107* and *myb9* Arabidopsis mutants displayed a significant reduction in suberin monomers and altered levels of other seed coat-associated metabolites. They also exhibited increased permeability, and lower germination capacities under osmotic and salt stress. AtMYB9 and AtMYB107 appear to synchronize the transcriptional induction of aliphatic and aromatic monomer biosynthesis and transport and suberin polymerization in the seed outer integument layer. Collectively, our findings establish a regulatory system controlling developmentally deposited suberin, which likely differs from the one of stress-induced polymer assembly recognized to date.

INTRODUCTION

The plant cuticle is an apoplastic lipophilic layer coating its entire aerial parts. It is characteristically comprised of a cutin polymer, consisting of long-chain fatty acids and glycerol, which is embedded with very long chain fatty acid waxes (Heredia, 2003; Bargel et al., 2006). The cutin polymer and embedded waxes are typically translucent, allowing photosynthesis, while also providing a strong water proofing barrier, and are thus crucial to the plant's terrestrial survival (Bargel et al., 2006; Isaacson et al., 2009; Chen et al., 2011a). While control of water movement can be considered the principal role of the cuticle, additional roles include structural support and protection against pathogen infection and herbivory (Isaacson et al., 2009; Chen et al., 2011a). In the event of wounding or damage to the surface, the plant produces suberin (Dean and Kolattukudy, 1976). This polymer is analogous to cutin, but consists of slightly longer chain length fatty acids as well as a polyphenol domain (predominantly ferulic esters) (Pollard et al., 2008; Schreiber, 2010; Beisson et al., 2012). Furthermore, the embedded waxes found in suberin often consist of alkyl ferulates, which are not typically found in cutin (Franke et al., 2005). This wound response suberin is typically brown and rough in appearance and can be seen on the surface of fruits, leaves, and stems, where it fulfills a similar role as the regular cuticle, although it is less elastic and typically a less efficient water barrier (Pollard et al., 2008; Lashbrooke et al., 2015a).

However, suberin is not exclusively produced as a wounding polymer; in fact, the majority of deposition of this polymer occurs during normal growth in the endodermis of roots, bark (exemplified in cork oak tree [*Quercus suber*]), seeds (specifically the seed coat), and specialized organs such as potato (*Solanum tuberosum*) tubers (Pollard et al., 2008; Schreiber, 2010). In such cases, its primary roles include regulation of water movement and protection from biotic stresses. It is within these tissues that the suberin research has been focused, yet in comparison to our understanding of cutin biosynthesis, less is known regarding the molecular mechanisms involved in suberin polymer assembly, particularly the transcriptional control of its biosynthetic pathway.

Thus far, several genes encoding enzymes involved in suberin biosynthesis have been described, including *β-KETOACYL-CoA SYNTHASEs* (*KCS2/DAISY* [Franke et al., 2009; Lee et al., 2009] and *KCS20* [Lee et al., 2009]), *fatty acid cytochrome P450 oxidases* (*CYP86A1* [Höfer et al., 2008] and *CYP86B1* [Compagnon et al., 2009; Molina et al., 2009]), *FATTY ACYL-COA REDUCTASEs* (*FARs*; Domergue et al., 2010; Vishwanath et al., 2013), and *GLYCEROL-3-PHOSPHATE ACYLTRANSFERASE5* (*GPAT5*; Beisson et al., 2007; Li et al., 2007), as well as those responsible for aromatic monomer inclusion, such as *ALIPHATIC SUBERIN*

[1] Current address: Department of Plant Systems Biology, VIB, 9052 Ghent, Belgium.
[2] Address correspondence to asaph.aharoni@weizmann.ac.il.
The author responsible for distribution of materials integral to the findings presented in this article in accordance with the policy described in the Instructions for Authors (www.plantcell.org) is: Asaph Aharoni (asaph.aharoni@weizmann.ac.il).
www.plantcell.org/cgi/doi/10.1105/tpc.16.00490

FERULOYL TRANSFERASE (*ASFT*; Gou et al., 2009; Molina et al., 2009). Recently, ATP BINDING CASSETTE G transporters (ABCG2, ABCG6, and ABCG20) have been shown to be required for suberin formation (Yadav et al., 2014). To date, no genes responsible for the extracellular polymerization of the suberin polymer or for the synthesis of the aromatic monomers have been described. While several transcription factors influencing plant cutin and wax formation have been identified (Isaacson et al., 2009; Oshima et al., 2013; Shi et al., 2011, 2013; Lashbrooke et al., 2015a, 2015b), only a single regulatory gene of suberin synthesis has been characterized. The recently described MYB factor AtMYB41 was demonstrated to be a positive regulator of suberin biosynthesis in *Arabidopsis thaliana* under stress conditions. Its overexpression was shown to activate ectopic suberin synthesis in multiple tissues (Kosma et al., 2014). *AtMYB41* expression was earlier found to be induced under drought, abscisic acid (ABA), and salt treatments, and it most likely plays a role in the plant's response to abiotic stresses (Cominelli et al., 2008).

Here, we aimed to identify genes associated with suberin polymer assembly and the transcriptional regulation of its biosynthetic pathway during plant development. The initial study of suberization in the wounded fruit skin surface of tomato (*Solanum lycopersicum*) and apple (*Malus x domestica*) led to the discovery of genes associated with developmentally regulated suberin deposition in multiple plant species. It appeared that the gene expression program as a consequence of russeting, a naturally occurring suberization phenomenon of apple surface (Khanal et al., 2013; Lashbrooke et al., 2015a), and suberization due to cuticular deficiency in tomato skin, is vastly analogous. Interrogating additional transcriptomics data sets associated with suberin formation uncovered a conserved gene expression signature associated with suberin monomer biosynthesis and polymer assembly. Central elements in this gene expression signature were *AtMYB107* and its homolog *AtMYB9*, a pair of Arabidopsis transcription factors that likely represent a clade of proteins playing a significant role in developmental suberin deposition in numerous plant species. Arabidopsis *myb107* and *myb9* T-DNA mutants displayed a significant reduction in particular seed coat aliphatics and aromatic components that are considered characteristics of the suberin polymer. The observed regulation by AtMYB107 and AtMYB9 of both the aliphatic and aromatic monomer biosynthesis pathways serves as an excellent base for studying the crosstalk between these pathways leading to suberin polymer formation. Hence, this work provides a stepping stone for investigations into the coordination between suberin biosynthesis, transport, and polymerization, in tissues specialized for suberin deposition, such as roots, seed coat, and tuber skin.

RESULTS

Silencing the Tomato *DEFECTIVE IN CUTICULAR RIDGES* Results in Intensive Suberization of the Tomato Fruit Surface

Earlier work showed that *DEFECTIVE IN CUTICULAR RIDGES* (*DCR*), a member of the BAHD family of acyltransferases, is required for incorporation of the most abundant cutin monomer into the polymeric structure of the Arabidopsis flower cuticle (Panikashvili et al., 2009). Notably, the same component, namely, 9(10),16-dihydroxyhexadecanoic acid (C16-9/10,16-DHFA), is the major cutin monomer of tomato, cherry (*Prunus avium*), and other fleshy fruit species (Kolattukudy, 2001; Peschel et al., 2007; Mintz-Oron et al., 2008). This similarity in cutin monomer composition of Arabidopsis petals and fleshy fruit, particularly tomato, suggested that DCR may play an important role in forming the tomato fruit surface. Expression analysis showed the tomato *DCR* ortholog (Solyc03g025320, displaying a 64% identity at the amino acid level to AtDCR; Supplemental Figure 1) is preferentially expressed in the skin tissue when compared with the flesh (i.e., pericarp) (Figure 1A). Furthermore, it is highly expressed at the early stages of fruit development and decreased sharply during maturation and ripening. This can be considered a typical expression profile of genes involved in fruit cuticle biosynthesis (Mintz-Oron et al., 2008).

To unravel the function of the tomato *DCR* ortholog, we silenced it in tomato plants. *SlDCR*-silenced tomato plants displayed several surface phenotypes, including organ fusions of leaves and flowers (Figure 1B; Supplemental Figure 2). However, the most striking phenotype was the fruit surface of the *SlDCR*-RNAi lines, which showed major cracking and browning, resembling the surface of potato tubers and increasing in intensity during fruit development, potentially indicative of suberin formation (Figure 1C). Light microscopy analysis suggested a reduction in cuticle deposition in the *SlDCR*-RNAi fruit when compared with the wild type (Supplemental Figure 3). Further analysis via scanning electron microscopy revealed microscopic cracks between cells, as well as larger fissures across the fruit surface (Figures 1C and D). Finally, transmission electron microscopy analysis showed what appear to be lipid inclusion bodies in the cytosol of the *SlDCR*-RNAi fruit epidermal cells (Figure 1E).

We subsequently performed chemical characterization of the brown, rough surface coating the *SlDCR*-RNAi fruit. The results showed a significant reduction in the majority of the quantified cutin monomers (Figure 1F), notably, a massive reduction in levels of C16-9/10,16-DHFA, the major tomato fruit cutin monomer (Mintz-Oron et al., 2008). This monomer typically accounts for an excess of 90% of the tomato fruit cutin polymer. Yet, several constituents displayed a significant increase in deposition, including the terminally hydroxylated and dicarboxylic fatty acids (C16-ω HFA and C16:0 dicarboxylic fatty acid, respectively) as well as the phenolic, ferulic acid. Significantly, these metabolic changes conform to the described differences between cutin and suberin (Pollard et al., 2008; Schreiber, 2010), suggesting suberization of the *SlDCR*-RNAi fruit surface. Furthermore, examination of the nonpolymerized wax component of the fruit cuticle identified a striking increase in ferulic esters, C18-C24 in length (Supplemental Table 1).

To examine if suberin-associated genes were activated in the epidermal cells of *SlDCR*-RNAi fruit, the expression of two putative tomato orthologs of well characterized suberin biosynthesis genes (*ASFT* [Molina et al., 2009] and *GPAT5* [Beisson et al., 2007]) were assayed. The skin tissue of mature green tomato fruit was studied, as *SlDCR*-RNAi fruit showed definitive signs of the putative suberin formation at this stage. The results revealed that expression of the only identified putative *ASFT* ortholog in tomato (Supplemental Figure 4) was dramatically increased in the skin of *SlDCR*-RNAi fruit (in excess of 350-fold; Figure 1G). Phylogenetic

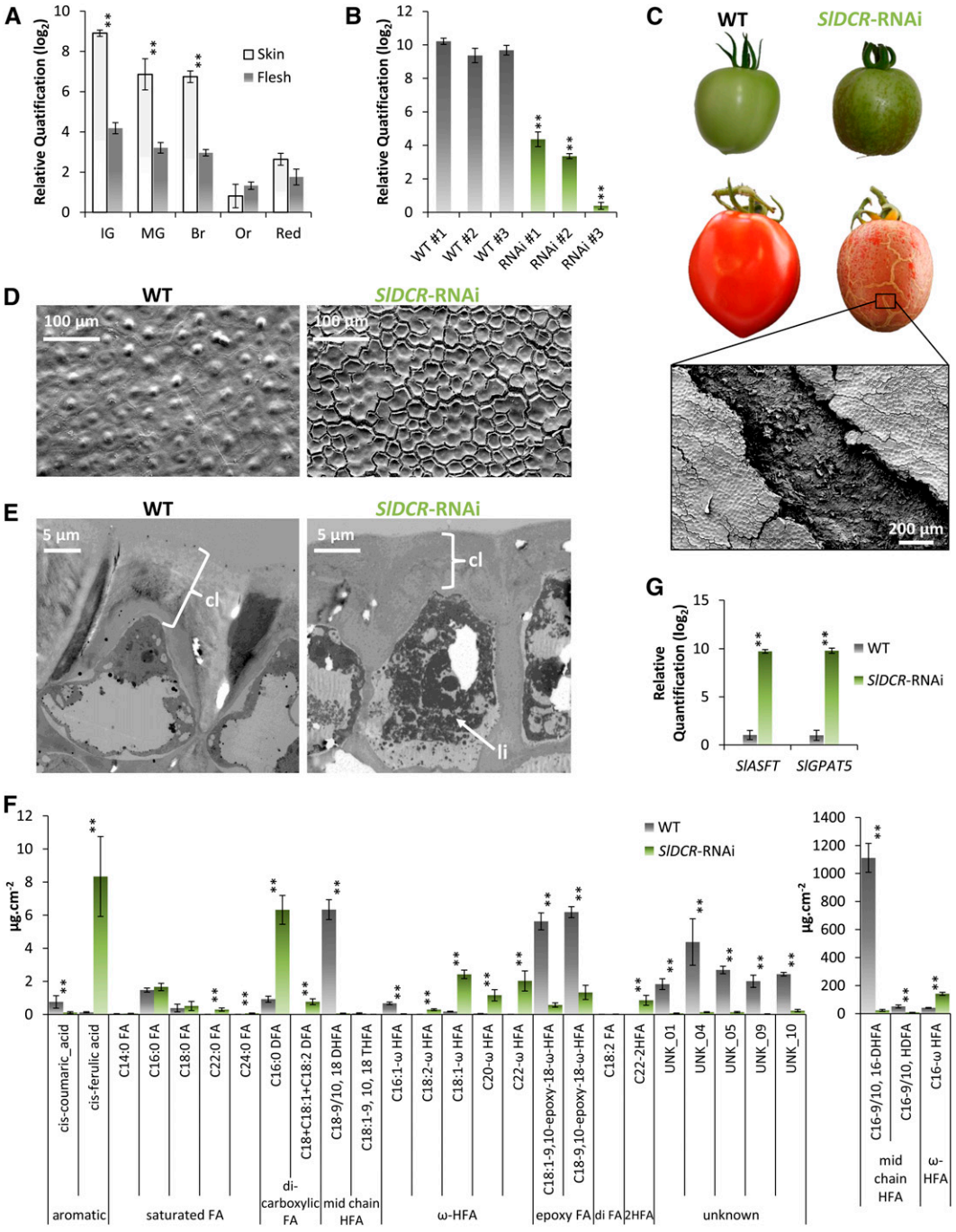

Figure 1. Silencing of *SlDCR* in Tomato Leads to Suberization of the Fruit Surface.

(A) Examination of *SlDCR* expression in developing tomato fruit via RT-qPCR shows a skin enriched expression profile. IG, immature green; MG, mature green; Br, breaker; Or, orange and red fruit stages. Error bars show SE ($n = 3$; **P value < 0.01, Student's *t* test).

(B) Confirmation of *SlDCR* silencing in mature green stage skin tissue via RT-qPCR of in transgenic lines (*SlDCR*-RNAi). Error bars show SE ($n = 3$; **P value < 0.01, Student's *t* test).

(C) Fruit surface phenotype of *SlDCR*-RNAi fruit at the mature green and red developmental stage. The disrupted epidermal layer of the *SlDCR*-RNAi fruit is revealed by scanning electron microscopy (see inset).

(D) Scanning electron microscopy analysis of red stage fruit surface shows microcracking between *SlDCR*-RNAi epidermal cells.

(E) Transmission electron microscopy analysis of fruit epidermal cell at the red development stage shows reduced cuticle layer (cl) and an increase in lipid inclusion bodies (li) in the cytosol of *SlDCR*-RNAi cells.

analysis of the tomato *GPAT* family revealed two potential GPAT5 orthologs (Supplemental Figure 5A and Supplemental Data Set 1). Expression analysis of GPAT family members in the *SlDCR*-RNAi fruit revealed that only *Solyc04g011600* (*SlGPAT5*) displayed a significantly altered expression, showing a >350-fold increase in expression compared with wild-type fruit skin (Figure 1G; Supplemental Figure 5B). Importantly, *SlGPAT4* and *SlGPAT6*, considered to be involved in cutin polymer formation (Yang et al., 2010; Chen et al., 2011b; Petit et al., 2016), showed no change in expression (Supplemental Figure 5).

The secondary nature of the suberin-like layer that coated the *SlDCR*-RNAi fruit (i.e., a response to wounding rather than a direct response to *SlDCR* silencing) was demonstrated through the partial covering of developing fruit with petroleum jelly. The jelly acted to simulate a properly functioning water-proofing cuticle. Regions of *SlDCR*-RNAi fruit covered with the jelly did not develop any visible suberization as compared with noncovered ones, thus decoupling the surface phenotype directly from *SlDCR* expression (Supplemental Figure 6).

The Russeting and Suberization of Apple Fruit Surface Resembles the Phenotype of *SlDCR*-Silenced Tomato Fruit

Following the results obtained from silencing *SlDCR* in tomato fruit, russeting, a similar phenomenon known in fruit was examined. In apple, russet is described as the suberization of the fruit surface that occurs developmentally following cuticular damage in some cultivars (Khanal et al., 2013; Lashbrooke et al., 2015a). A regular skinned clone of the apple cultivar Golden Delicious ('Reinders') was analyzed in conjunction with a clone deriving from a somatic mutation for this cultivar that shows highly russeted fruits ('Rugiada') (Figure 2A). As in the case of *SlDCR*-RNAi tomato, the surface of the 'Rugiada' apple fruit appeared brown, rough, and cracked. Light microscopy and scanning electron microscopy analysis highlighted the dramatically reduced cuticle of these russeted apples leading to this phenotype (Figure 2B; Supplemental Figure 7).

Chemical analysis of the depolymerized cuticle polymer was subsequently performed and revealed a number of striking changes between the two apple clones (Figure 2C). The russet apple skin tissue showed a drastic reduction in the mid-chain hydroxylated fatty acid, C16-9/10,16-DHFA, as well as the terminal hydroxylated fatty acid, C16-ω-HFA, and the epoxy fatty acid, C18:1-9,10-epoxy-19-ω-HFA. This was coupled with massive increases in C20- and C22-ω-HFAs, as well as the saturated C22:0 FA. Significantly, an increase in the phenolics, benzoic acid, ferulic acid, and cinnamic acid was also observed. These metabolic changes are indicative of suberin formation (Franke et al., 2005; Pollard et al., 2008) and provide a strong indication for the presence of this polymer in the surface of russeted apples.

Analogous Gene Expression Profiles Detected in the Surface Tissues of Russeted Apple and *SlDCR*-Silenced Tomato Fruit

The similarities between transcriptional changes occurring during russet development in apple and the suberization phenotype of *SlDCR*-RNAi fruit skin were subsequently investigated. Transcriptome assays of russeted apple included the analysis of both skin and flesh tissues in the regular skinned 'Reinders' and the russeted 'Rugiada' clones at five fruit developmental stages (Supplemental Data Set 2). Stage-specific enrichment for gene expression in the russeted skin samples (at least 2-fold increase versus regular skin) was subsequently determined and genes showing enrichment in multiple stages identified (see Methods for details). Expression of 1302 genes was found to be russet skin enriched in at least 75% of the stages analyzed (three out of four stages or four out of five stages), and of these genes, 486 showed russet skin expression enrichment in all stages analyzed.

In tomato, the transcriptome of wounded fruit skin tissue derived from the *SlDCR*-RNAi lines was compared with wild-type tomato skin tissue (both at the mature green stage). A set of 504 genes were significantly upregulated in the *SlDCR*-RNAi skin tissue (P value < 0.05) (Supplemental Data Set 3). Cross-comparison of the apple and tomato data sets (i.e., 486 tomato versus 504 apple genes) identified a set of 70 putatively orthologous gene groups comprising 90 tomato genes and 86 apple genes that were enriched for expression in the suberized surfaces of both the *SlDCR*-RNAi tomato fruit and russeted apple (Supplemental Table 2). Gene Ontology enrichment analysis of the orthologous gene list found a significant enrichment (P value < 0.001) for biosynthetic processes involved in aromatic compounds, phenylpropanoids, suberin, fatty acids, and lignin (Supplemental Figure 8).

Closer examination of the common orthologous genes in the apple and tomato data sets revealed that the known suberin biosynthesis genes (*ASFT*, *GPAT5*, and *CYP86B1*) displayed almost exclusive expression in the suberized apple and tomato skin tissues (Figure 3; Supplemental Data Sets 2 and 3). Further genes upregulated in the suberized skins of tomato and apple with a potential role in suberin biosynthesis included genes involved in phenylpropanoid biosynthesis, *4-COUMARATE:COA LIGASE5* (*4CL5*), *FERULIC ACID 5-HYDROXYLASE1* (*FAH1*), and *CAFFEOYL COA DEPENDENT O-METHYLTRANSFERASE1* (*CCoAOMT*); fatty acid biosynthesis, *FATTY ACYL-ACP THIOESTERASES B* (*FATB*); suberin monomer transport and polymerization, *ABCG20*, *GLYCOSYLPHOSPHATIDYLINOSITOL-ANCHORED LIPID PROTEIN TRANSFER5* (*LTPG5*) and a number of GDSL-motif esterase/acyltransferase/lipase genes; and transcriptional regulators, *NAC DOMAIN CONTAINING PROTEIN38* (*NAC38*), *MYB DOMAIN PROTEINs* (*MYB67* and *MYB107*), and *WRKY DNA BINDING PROTEIN28* (*WRKY28*) (Figure 3; Supplemental Table 2).

Figure 1. (continued).

(F) Chemical analysis via gas chromatography-mass spectrometry (GC-MS) of the fruit surface polymer in *SlDCR*-RNAi lines shows a massive decrease in C16-9/10,16-DHFA and an increase in monomers typically found in suberin polymer. Error bars show SE ($n = 4$; **P value < 0.01, Student's t test).
(G) Expression analysis (RT-qPCR) shows a massive increase in expression of *SlASFT* and *SlGPAT5* (over 350-fold) in *SlDCR*-RNAi mature green fruit skin. Error bars show SE ($n = 3$; **P value < 0.01, Student's t test).

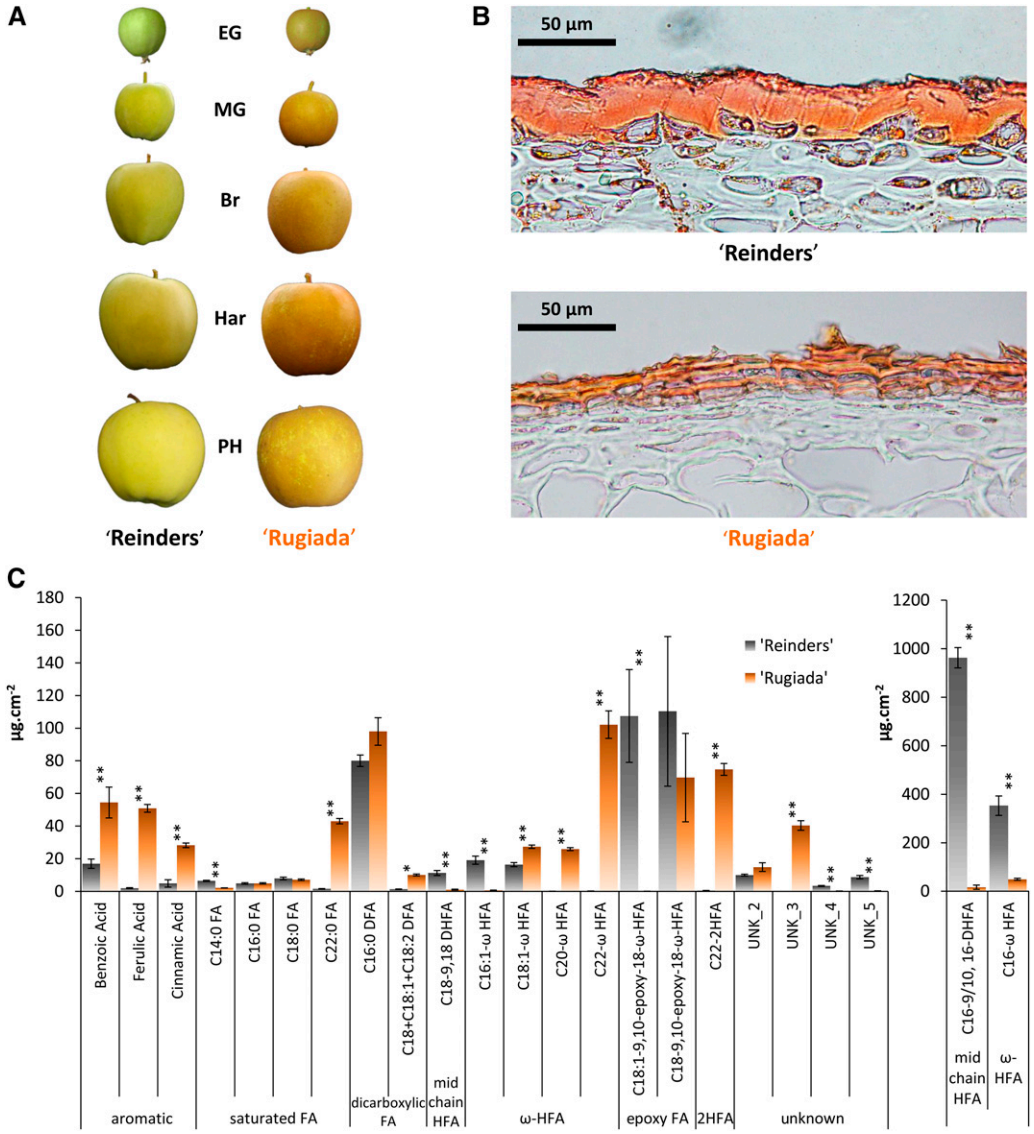

Figure 2. Surface Phenotype and Chemical Composition of Apple Russet.

(A) Two Golden Delicious apple clones were analyzed: the normal skinned 'Reinders' clone and the russeted 'Rugiada' clone. 'Rugiada' displays a rough, brown, and cracked fruit surface. EG, early green; MG, mature green; Br, breaker; Har, harvest; PH, postharvest fruit stages.

(B) Light microscopy of the epidermal layer of harvest stage fruit from 'Reinders' and 'Rugiada' using the lipid stain Sudan IV shows a dramatic reduction in cuticle deposition in the latter clone.

(C) Chemical analysis via GC-MS of the surface polymer of these two clones highlights the dramatic reduction in C16-9/10,16-DHFA and C16-ω-HFA monomers of 'Rugiada', while an increase in longer chain length C20- and C22-ω-HFA is observed, together with an increase in aromatics. Error bars show SE (n = 4; *P value < 0.05, **P value < 0.01, Student's t test).

Comparative Transcriptome Analysis Reveals a Multispecies Gene Expression Signature for Suberin Biosynthesis

The striking similarities in gene expression patterns between suberized tomato and russeted apple tissues provided a list of candidate genes likely involved in suberin formation. To increase the robustness of this comparative coexpression comparison analysis, conserved coexpression patterns across additional plant species and tissues were examined. To this end, a collection of multitissue transcriptome data sets was identified from several species, each possessing an association with suberin deposition. In addition to (1) apple (i.e., russet clone) and (2) tomato (i.e., *SlDCR*-RNAi) fruit transcriptome data sets described above, this collection included gene expression data sets of (3) seed tissues during development in Arabidopsis (Le et al., 2010), (4) all major organs of grapevine (*Vitis vinifera*) (Fasoli et al., 2012), (5) multiple organs of tomato (Tomato Gene Consortium, 2012), (6) potato (Xu et al., 2011), and (7) the roots

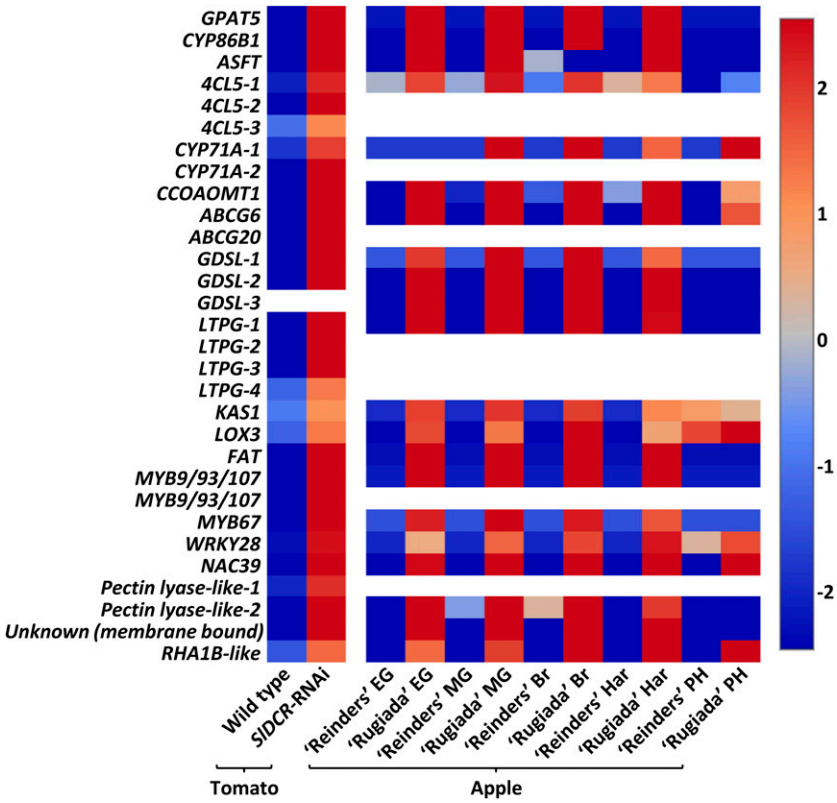

Figure 3. Orthologous Genes Upregulated in Both the Suberized Fruit Skin Tissues of *SlDCR*-RNAi Tomato and Russeted Apple.

Genes upregulated in *SlDCR*-RNAi compared with the wild type and in the russeted 'Rugiada' clone compared with the regular skinned 'Reinders' were depicted in a heat map. For a full list of identified genes and the corresponding expression patterns, see Supplemental Data Sets 2 and 3 and Supplemental Table 2. Bar indicates $\log_2$(fold change) of gene expression centered on the mean of expression for each gene. EG, early green; MG, mature green; Br, breaker; Har, harvest; PH, postharvest fruit stages.

of rice (*Oryza sativa*) during waterlogging (Shiono et al., 2014). Each of the seven individual transcriptome data sets was subsequently used for coexpression analysis in which putative orthologs of three Arabidopsis genes known for their direct involvement in suberin biosynthesis (i.e., *GPAT5* [Beisson et al., 2007], *ASFT* [Molina et al., 2009], and *CYP86B1* [Compagnon et al., 2009]) were used as baits (i.e., multiple gene coexpression; see Methods for details). These genes were selected based on their orthology to the known and functionally characterized (i.e., Arabidopsis) genes and their expression patterns in the respective data sets (Supplemental Figure 9).

The output of coexpression analysis in each of the seven transcriptome data sets was used to determine orthology between the coexpressed genes (Supplemental Data Set 4). Consequently, 1454 gene ortholog groups were identified. The coexpressed orthologs were ranked based on their frequency of occurrence in the seven data sets; two sets of orthologs were found in all seven lists, three in six, 11 in five, and 10 in four experiments (26 in total). This list of 26 genes was considered as a "suberin gene expression signature," spanning multiple tissues and species. The suberin signature included several genes previously shown to be involved in various steps of suberin formation as well as those not linked directly with suberin formation, but associated with fatty acid synthesis, lignin/phenylpropanoid metabolism, transport, extracellular polymerization, and transcriptional regulation (Figure 4, Table 1).

Identification of a MYB Transcription Factor Clade Linked to Suberin Biosynthesis across Multiple Plant Species

Examination of the two ortholog groups of genes identified in all seven coexpression data sets revealed that they putatively encode (1) a clade of MYB factors containing the Arabidopsis MYB9, MYB93, and MYB107 proteins (Figure 5) and (2) a clade GDSL-motif esterases (Supplemental Figure 10 and Supplemental Data Set 5). Expression profiles of the genes encoding MYB proteins from Arabidopsis (AtMYB107 and AtMYB9, AT3G02940 and AT5G16770), tomato (SlMYB93, Solyc04g074170), apple (MdMYB53, MDP0000145757), grape (VvMYB107, VIT_16s0039g01710), potato (StMYB93, PGSC0003DMP400011365), and rice (OsMYB93, LOC_Os03g27090) are shown with the bait genes (*GPAT5*, *ASFT*, and *CYP86B1*) in Supplemental Figures 9A to 9G and illustrate the conservation of expression pattern of these regulators with the known suberin biosynthesis genes. Phylogenetic analysis of the identified GDSL-motif esterases found the clade to be a close relative of the cutin synthase (CUS) clade (Yeats et al., 2012, 2014)

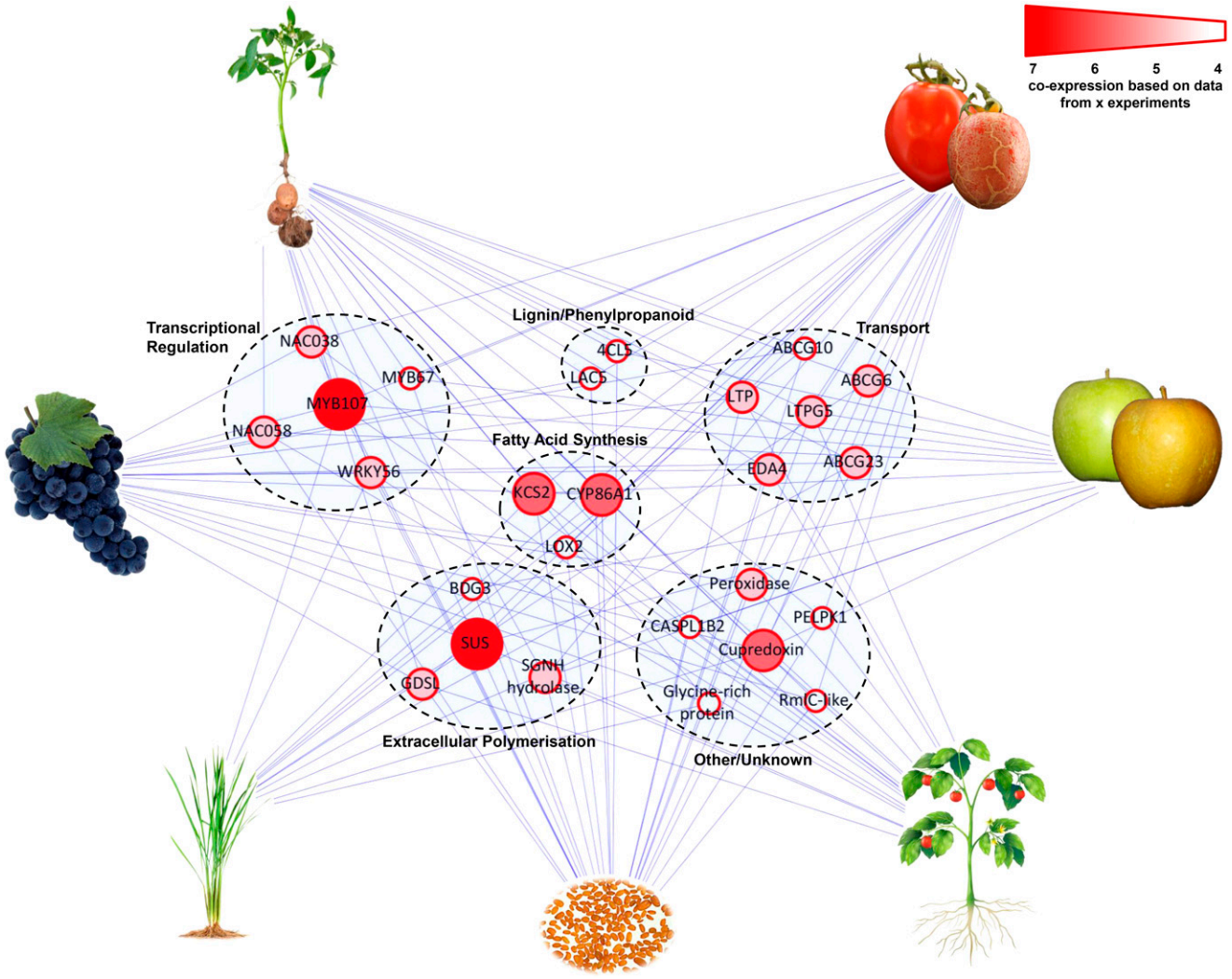

Figure 4. A Multispecies Gene Expression Signature for Suberin Biosynthesis.

Orthologous genes identified through the multi-species suberin gene coexpression analysis are represented graphically. Genes found to be coexpressed with baits representing known suberin synthesis genes were identified in seven data sets and compared for orthology. Clockwise from top right the images represent transcriptomics data sets that examined expression in *SlDCR*-RNAi versus wild-type fruit skin tissues, russeted versus regular skinned apples surface tissues, multiple tissue types from whole tomato plant, Arabidopsis seeds tissues, waterlogged rice roots versus wild-type roots, whole grapevine plant tissues, and whole potato plant tissues. Edges (blue lines) represent presence of the corresponding ortholog to the expression data set, while nodes (red circles) represent orthologous gene groups. Bar indicates the number of experiments in which the orthologous gene group was identified (i.e., four, five, six, or seven coexpression experiments; seven out of seven analyses is represented by the largest and most intensely red colored circle). Orthologs were grouped based on their proposed function. For respective gene IDs and details of the coexpression parameters, see Table 1 and Supplemental Table 6, respectively.

of GDSL-motif esterases (Supplemental Figure 10 and Supplemental Data Set 5). We therefore proposed that proteins of this newly identified clade possess an analogous role to CUS proteins yet in suberin polymer assembly and termed them SUBERIN SYNTHASE (SUS) proteins.

Phylogenetic investigation of the MYB transcription factor candidates identified through the multispecies coexpression analysis was performed together with related Arabidopsis proteins. All factors were found to be positioned in one of two previously defined MYB family subgroups (Dubos et al., 2010) (i.e., subgroup 10 or 24; Figure 5). Sequence analysis of the members of these subgroups identified common and yet undescribed protein motifs (Figure 5), suggesting that subgroups 10 and 24 could be defined as one single clade. Specifically, analyzing for conserved motifs located in these proteins at their C terminus identified two neighboring motifs (termed here SUB-I and SUB-II; located C-terminal to the R3-MYB repeat), which were present in the MYB proteins from all six investigated plant species examined. A third motif, found adjacent to the C terminus (termed SUB-III), was found to be present in five species with the exception of the monocotyledonous rice ortholog (OsMYB93)

Table 1. Multispecies Gene Expression Signature Identified for Suberin Biosynthesis through Coexpression Analysis

Short Name	Ass. Exp.	Full Name	Function	Reference for Function
MYB107	7	MYB DOMAIN PROTEIN107	Transcriptional regulator	This study
SUS	7	SUBERIN SYNTHASE	Extracellular polymerization	Inferred through similarities with characterized clade members (Yeats et al., 2012, 2014)
DAISY/KCS2	6	3-KETOACYL-COA SYNTHASE2	Fatty acid synthesis	Franke et al. (2009); Lee et al. (2009)
CYP86A1/ HORST	6	CYTOCHROME P450 86A1	Fatty acid synthesis	Höfer et al. (2008)
Cupredoxin	6	Cupredoxin superfamily protein	Unknown	
ABCG20	5	ATP-BINDING CASSETTE G20	Transport	Inferred through the characterization of knockout mutants (Yadav et al., 2014)
LTPG5	5	GLYCOSYLPHOSPHATIDYLINOSITOL-ANCHORED LIPID PROTEIN TRANSFER5	Transport	Inferred through similarities with the characterized LTPG1 (Debono et al., 2009) and the characterization of LTPG knockout mutants (Edstam and Edqvist, 2014)
NAC038	5	NAC DOMAIN CONTAINING PROTEIN38	Transcriptional regulator	Uncharacterized member of NAC clade
WRKY56	5	WRKY DNA-BINDING PROTEIN56	Transcriptional regulator	Uncharacterized member of WRKY clade
LTP	5	Bifunctional inhibitor/lipid-transfer protein/seed storage 2S albumin superfamily protein	Unknown/hypothesized lipid transport	Inferred through similarities with characterized clade members (Li-Beisson et al., 2013)
NAC058	5	NAC DOMAIN CONTAINING PROTEIN58	Transcriptional regulator	Uncharacterized member of NAC clade
Peroxidase	5	Peroxidase superfamily protein	Response to oxidative stress	Inferred through similarities with characterized clade members (Welinder et al., 2002)
SGNH	5	SGNH hydrolase-type esterase superfamily protein	Lipid metabolism	Inferred through similarities with characterized clade members (Li-Beisson et al., 2013)
GDSL	5	GDSL-motif esterase/acyltransferase/ lipase	Hypothesized extracellular polymerization	Inferred through similarities with characterized clade members (Yeats et al., 2012, 2014)
ABCG23	5	ATP-BINDING CASSETTE G23	Transport	Inferred through similarities with characterized clade members (Yadav et al., 2014)
EDA4	5	EMBRYO SAC DEVELOPMENT ARREST4	Unknown/hypothesized lipid transport	Inferred through similarities with characterized clade members (Li-Beisson et al., 2013)
LOX2	4	LIPOXYGENASE2	Fatty acid synthesis	Mochizuki et al. (2016)
RmlC-like cupins	4	RmlC-like cupins superfamily protein	Unknown/hypothesized manganese binding	Yang et al. (2008)
4CL5	4	4-COUMARATE:COA LIGASE5	Phenylpropanoid/lignin synthesis	Hamberger and Hahlbrock (2004); Costa et al. (2005)
LAC5	4	LACCASE5	Lignin metabolism	Inferred through similarities with characterized clade members (Zhao et al., 2013; Schuetz et al., 2014)
ABCG10	4	ATP-BINDING CASSETTE G10	Transport	Inferred through similarities with characterized clade members (Yadav et al., 2014)
MYB67	4	MYB DOMAIN PROTEIN 67	Transcriptional regulator	Uncharacterized member of MYB clade
BDG3	4	BODYGUARD3	Hypothesized extracellular polymerization	Shi et al. (2011)
CASPL1B2	4	CASP-LIKE PROTEIN 1B2	Unknown/transmembrane scaffold	Roppolo et al. (2014)
Glycine-rich protein	4	Glycine-rich protein	Unknown	
PELPK1	4	PRO-GLU-LEU-PRO-LYS1	Regulator of germination	Rashid and Deyholos (2011)

Ortholog groups of genes identified in coexpression data sets (with known suberin genes as baits) described in the text from tomato, apple, Arabidopsis, potato, grape, and rice. A graphical representation of the data can be seen in Figure 4 and gene IDs retrieved from Supplemental Table 3. Ass. Exp., associated experiments.

(Figure 5; Supplemental Data Set 6). Examining the MYB factors from the adjacent subgroups (i.e., 9 and 11), which contain the previously reported ABA/suberin (MYB41) and cutin regulators (MYB16 and MYB106) for these newly identified motifs returned no hits. Importantly, AtMYB9, not identified in the coexpression analysis previously due to a spike in gene expression in the chalaza endosperm, but which otherwise displays an expression pattern consistent with suberin deposition in the developing Arabidopsis seed (Figure 6; Supplemental Figure 9), also contained the identified motifs (Figure 5). Hence, it was also considered further as a candidate for transcriptional regulation of the suberin assembly pathway.

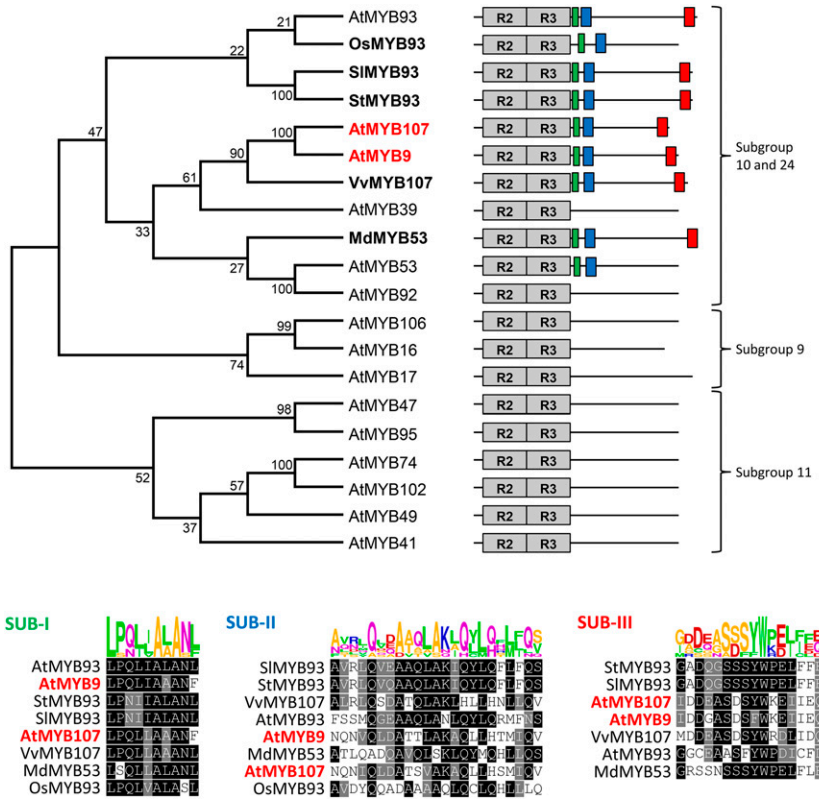

Figure 5. Identification of a Clade of MYB Factors Likely Involved in Suberin Formation across Multiple Species.

Molecular phylogenetic analysis of Arabidopsis MYB factors from subgroups 9, 10, 11, and 24 was performed together with the MYB factors identified in this study to be expressed in suberin forming tissues of other species (in bold). While subgroups 9 and 11 form separate clades, division of subgroups 10 and 24 was not clearly resolved. Protein domain analysis identified three C-terminal motifs specific to this combined clade that may be involved in regulation of suberin formation (SUB-I, SUB-II, and SUB-III). The motifs are marked on top of the gene structure downstream of the indicated R2-R3 domains characteristic of plant MYB proteins. Detailed representation of the identified motifs is shown in full below. AtMYB9 and AtMYB107 are highlighted in red and bold text. ClustalW and MEGA6 software were used to align the proteins and compute the neighbor-joining tree with significance percentages (bootstrap values out of 1000). The alignment used to generate the phylogeny is presented in Supplemental Data Set 6.

To confirm the association of the candidate Arabidopsis MYB transcription factors (i.e., *AtMYB107* and *AtMYB9*) with suberin biosynthesis and deposition their corresponding T-DNA knockout lines were characterized (Table 1; Supplemental Table 3). Furthermore, knockout lines were also identified for additional Arabidopsis genes included in the suberin gene expression signature. After screening for homozygous insertions, lines representing 11 of the 16 genes found coexpressed in five or more transcriptome experiments (up to seven data sets; Figure 4, Table 1) were analyzed for seed permeability. Significantly, homozygous lines for the Arabidopsis ortholog for SUS could not be recovered (only heterozygous lines were found). Seeds of homozygous lines were examined in a tetrazolium chloride seed staining assay that is commonly used in Arabidopsis to identify an increase in seed permeability, which in turn may indicate altered suberin deposition in the seed coat. Tetrazolium staining of control lines (known suberin mutants: *asft*, *gpat5*, and *cyp86b1*) showed similar results to those reported previously; both *asft* and *gpat5* knockouts showed strong staining, while *cyp86b1* was not significantly stained (Beisson et al., 2007; Compagnon et al., 2009; Molina et al., 2009) (Supplemental Figure 11). Assays performed on seeds derived from *myb107* and *myb9* lines displayed a highly significant increase in staining when compared with the wild type ($P < 0.005$; Figure 6; Supplemental Figures 11 and 12). Importantly, significant staining was also observed for the *abcg20* (*at5g13580*) and *nac38* (*at2g24430*) mutants (Supplemental Figure 11). AtABCG20 has recently been implicated in the transport of suberin monomers (Yadav et al., 2014). Transcript profiling data of the genes mentioned above demonstrated that expression of these genes during seed development was entirely confined to the seed coat at the mature green stage of seed development (Supplemental Figure 9). *AtMYB9* expression deviates from this profile as mentioned earlier, showing expression in the chalaza endosperm at the heart stage of development, while *NAC38* appears to have a higher background expression in non-seed coat tissues. In addition, RT-qPCR expression analysis of seeds from the mature green stage until dormant stage indicates a spike in gene expression for AtMYB107, while the inverse was observed for AtMYB9 (Supplemental Figure 13).

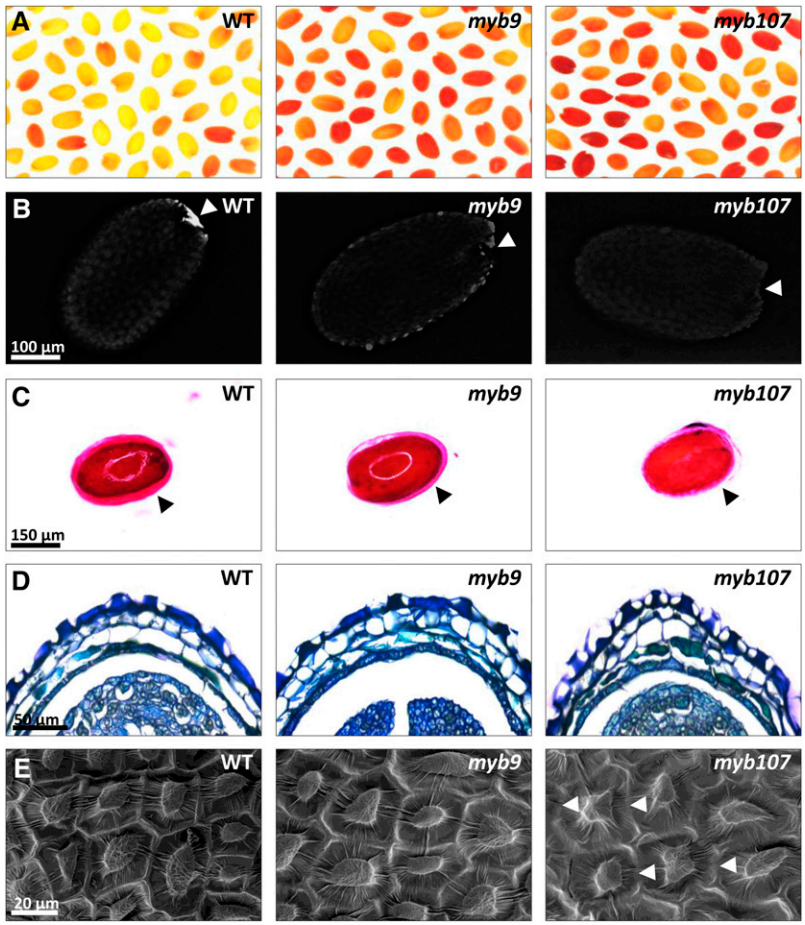

Figure 6. Seed Coat Phenotypes of *myb107* and *myb9* Arabidopsis Mutant Lines.

(A) Tetrazolium salt penetration assays for seeds of Arabidopsis T-DNA insertion lines identified an increase in seed permeability (resulting in red staining of seeds) for *myb107* and *myb9* mutant lines when compared with the Col-0 wild-type control.
(B) Autofluorescence of suberin in mature Arabidopsis seeds when excited at 365 nm shows a decrease in fluorescence in the hilum region (arrowheads) of the mutant seeds.
(C) Ruthenium red staining of seed mucilage highlights the decreased mucilage layer (arrowheads) of *myb107* and *myb9* seeds.
(D) Histological sections of seed coats stained with toluidine blue O shows the relative disorganization of the integument layers in the *myb107* seed coat.
(E) Scanning electron microscopy images of seed coat surface structure and columella cells identifies gaps at the columella cell borders of *myb107* seeds (arrowheads).

Seeds from *myb107* and *myb9* lines were subsequently examined in more detail for seed coat phenotypes. Autofluorescence of the suberin polymer when excited at 365 nm was found to be decreased in the seeds of both *myb107* and *myb9* lines when compared with wild-type Columbia ecotype (Col-0) seeds (Figure 6B). Staining with ruthenium red indicated that the mucilage layer produced by *myb107* and *myb9* seeds was thinner when compared with wild-type seeds (Figure 6C). Interestingly, both observations were more pronounced in the seeds of *myb107* lines. Histological sectioning and observation of wild-type and *myb9* seeds displayed clear seed coat layers of the inner and outer integuments, while the seed coat of *myb107* seeds exhibited morphological rearrangements (Figure 6D). Closer examination of the seed coat surfaces by scanning electron microscopy found that *myb9* seeds display a similar size and shape in terms of columella heaps when compared with the wild-type seeds; however, *myb107* seeds exhibited observable gaps in the borders between columella cells (Figure 6E; Supplemental Figure 14).

MYB107 and MYB9 Are Required for Suberin-Associated Gene Expression in the Course of Arabidopsis Seed Development

The T-DNA insertion in the *myb107* line (SAIL_242_B04.V1) is situated in the 5′ untranslated region of *AtMYB107*, causing a significant downregulation of *AtMYB107* expression in seeds at the mature green stage (up to 40-fold) (Supplemental Figure 13). With regards to the *myb9* line (GK-661C10-023861), the T-DNA insertion is slightly upstream of the 5′ untranslated region and results in an 8-fold downregulation of *AtMYB9* expression (Supplemental Figure 13).

Notably, expression analysis showed that *AtMYB107* is upregulated in *myb9*, while no significant change in expression of *AtMYB9* was detected in the *myb107* lines (Supplemental Figure 13).

Mature green stage seeds of the *myb9* and *myb107* mutants and wild-type plants were subjected to transcriptome analysis (i.e., RNA-seq; Supplemental Data Set 7). When compared with the wild type, 1074 and 572 genes were downregulated in *myb9* and *myb107* seeds, respectively (Supplemental Data Set 7). A total of 312 genes were found to be significantly downregulated in both *myb9* and *myb107* mutant seeds. A selected number of genes are provided in Table 2 and include those involved in both aliphatic and aromatic metabolic pathways associated with suberin formation. Genes potentially linked with suberin biosynthesis found to be downregulated in both *myb9* and *myb107* seeds include those encoding SUS (the putative suberin synthase); an SGNH hydrolase-type esterase superfamily protein (likely involved in lipid metabolic processes; Li-Beisson et al., 2013); CASP-LIKE PROTEIN 1B2 (CASPL1B2, showing strong homology to CASP proteins involved in casparian strip metabolism); LACCASE3 (a member of the laccase family of which LACCASE4 has been demonstrated to be involved in lignin metabolism; Zhao et al., 2013; Schuetz et al., 2014); DIHYDROFLAVONOL 4-REDUCTASE-LIKE1 (DFR-like1; involved in phenylpropanoid metabolism and previously linked to pollen wall development and seed production (Lallemand et al., 2013); and LUPEOL SYNTHASE5 (LUP5; a multifunctional triterpene synthase; Ebizuka et al., 2003). While genes downregulated in *myb107* seeds (but not *myb9* seeds) encode GPAT5 and ASFT (known to act in suberin formation); 3-KETOACYL-COA SYNTHASE17 (KCS17; a very-long-chain fatty acid synthase); 4-COUMARATE:COA LIGASE5 (4CL5; involved in phenylpropanoid metabolism); and GLYCOSYLPHOSPHATIDYLINOSITOL-ANCHORED LIPID PROTEIN TRANSFER5 (LTPG5; a homolog to the lipid transporter LTPG1; Debono et al., 2009; Edstam and Edqvist, 2014). Finally, the gene encoding CYP86A1, characterized for its involvement in suberin monomer biosynthesis, was downregulated in *myb9* seeds (but not *myb107* seeds).

Levels of Aliphatic and Aromatic Suberin Constituents and Epicuticular Waxes Are Reduced in the Seeds of *myb107* and *myb9* Arabidopsis Mutants

In subsequent experiments, mature dry seeds of the *myb107* and *myb9* mutant lines were analyzed for the chemical composition of the seed coat polyester layer (Figure 7). Both lines showed a significant reduction in constituents of the seed coat polymer that are considered characteristic elements of the suberin polymer (Pollard et al., 2008). These included aliphatics such as C20, C22, and C24 terminal hydroxyl fatty acids, C24 dicarboxylic fatty acids, C18 and C20 fatty alcohols, and the aromatic molecule ferulic acid. Quantification of epicuticular wax monomers extracted from wild-type, *myb9*, and *myb107* seed coats showed striking reductions of primary fatty acids and fatty alcohols in samples of both mutant lines, while significantly lower levels of C31 alkane were observed in samples of *myb107* mutant seeds (Supplemental Figure 15). Additionally, chemical analyses showed that *myb107* mutant seeds accumulated significantly

Table 2. Selection of Genes Showing Downregulated Expression in Mature Green Stage Seeds of the *myb9* and/or *myb107* Arabidopsis Mutants Compared with Wild-Type Ones

			Gene Expression Fold Change (log_2) versus the Wild Type	
Gene ID	Gene Name	Gene Function	*myb9*	*myb107*
AT3G02940	*MYB107*	Transcriptional regulator	1.02*	−4.69*
AT5G16770	*MYB9*	Transcriptional regulator	−2.46*	−0.65*
AT3G11430	*GPAT5*	Acyltransferase (glycerol)	−0.68	−1.55
AT5G41040	*ASFT*	Acyltransferase (ferulate)	0.01*	−1.22*
AT5G23190	*CYP86B1*	Fatty acid hydroxylation	−0.18*	−0.75#
AT2G23540	*SUS*	Polymerization of suberin	−1.57#	−1.69*
AT5G58860	*CYP86A1*	Fatty acid hydroxylation	−1.87	−0.79
AT4G34510	*KCS17*	Fatty acid elongation	−0.54	−2.35
AT5G37690	*SGNH*	Lipid metabolism	−5.37	−3.03
AT3G21230	*4CL5*	Phenylpropanoid metabolism	0.21*	−1.24*
AT5G52320	*CYP96A4*	Lipid metabolism	−1.48	−1.48
AT4G20390	*CASPL1B2*	Unknown/transmembrane scaffold	−2.02*	−2.01*
AT2G30210	*LACCASE3*	Lignin metabolism	−4.02	−1.77
AT4G35420	*DFR-like1*	Pollen exine formation	−2.27	−1.86
AT1G09550	*PAE*	Unknown	−2.87	−1.85
AT1G66960	*LUP5*	Triterpenoid metabolism	−2.62	−2.62
AT3G22600	*LTPG5*	Lipid transport	−0.69	−1.39

Genes were selected from large-scale transcriptome data. GPAT5, GLYCEROL-3-PHOSPHATE ACYLTRANSFERASE5; ASFT, ALIPHATIC SUBERIN FERULOYL TRANSFERASE; KCS17, 3-KETOACYL-COA SYNTHASE17; SGNH, SGNH hydrolase-type esterase; 4CL5, 4-COUMARATE:COA LIGASE5; CASPL1B2, CASP-LIKE PROTEIN 1B2; DFR-like1, DIHYDROFLAVONOL 4-REDUCTASE-LIKE1; PAE, pectinacetylesterase; LUP5, LUPEOL SYNTHASE5; LTPG5, GLYCOSYLPHOSPHATIDYLINOSITOL-ANCHORED LIPID PROTEIN TRANSFER5; SUS, SUBERIN SYNTHASE. *, RT-qPCR experiments confirmed results seen in RNA-seq; #, RT-qPCR experiment is contrary to results seen in RNA-seq.

higher levels of aromatic amino acid precursors, soluble proanthocyanidins, and flavonols (Supplemental Figure 15). Finally, profiling of the mutant seeds for ABA and its derivatives found that while levels of these metabolites were not significantly different in *myb9* seeds, *myb107* seeds exhibited significant decreases in the levels of (−)-dihydrophaseic acid, phaseic acid, and ABA glucose ester and a significant increase in the level of neophaseic acid (Supplemental Figure 16).

Seeds of *myb107* but Not *myb9* Mutant Lines Exhibit Decreased Germination Rates under Osmotic and Salt Stress

In a final experiment, germination assays were performed with *myb107* and *myb9* mutant seeds under various levels of osmotic stress (Figure 8; Supplemental Figure 17). Under normal conditions (0.5% Murashige and Skoog medium/sucrose), both mutant seeds exhibited similar germination rates as the wild-type seeds, attaining >90% germination 7 d after imbibition (Figure 8A). Comparable germination rates were observed among seeds from the three genotypes under mild osmotic stress (150 mM mannitol; Figure 8B); however, under severe osmotic conditions (300 mM mannitol), *myb107* seeds exhibited germination rates 10 to 15% lower when compared with wild-type and *myb9* seeds (Figure 8C). A similar trend was observed for seeds under mild salt stress (100 mM NaCl), where *myb107* seeds exhibited a 20 to 30% lower germination rate when compared with wild-type seeds (Figure 8D).

DISCUSSION

In specialized plant tissues, such as the periderm layers of the cork oak tree and potato tuber skin, the deposition of suberin is a developmentally regulated process that occurs during cell wall differentiation. Yet, suberization is one of the hallmarks of wound injury and is well known to occur in cases of abiotic and biotic stress conditions. This is highlighted by the recent discovery that *ATMYB41* is involved in the ABA-mediated plant response and suberin formation (Cominelli et al., 2008; Lippold et al., 2009; Kosma et al., 2014). In potato tuber, native and wound periderms are similar in composition, although the wound periderm is enriched with wax alkyl ferulates and is more permeable to water (Schreiber et al., 2005). Interestingly, silencing of *SlDCR* in tomato resulted in severe damage to the fruit skin and a coating of a brown, rough material superficially resembling the potato tuber periderm. Indeed, chemical analysis of the tomato surface identified the presence (or increase) in signature molecules of suberin polymer, including terminally hydroxylated and dicarboxylic fatty acids as well as ferulate. Furthermore, a dramatic increase in unpolymerized ferulate esters was found in the wax fraction of the fruit cuticle. This suggests both a shift to suberin monomer formation, but also inadequate polymerization of the produced monomers as observed in the potato wound healing response (Bernards and Lewis, 1992; Schreiber et al., 2005). The metabolic change was coupled to a dramatic increase in the transcript abundance of the tomato orthologs of *GPAT5* and *ASFT*, genes known to play a central role in suberin formation. Despite the previous characterization of several tomato fruit cuticular mutants, this phenotype has not been previously described. For instance, the *cutin deficient1* (*cd1*), *cd2*, and *cd3* altered in cutin biosynthesis (*cd1* and *cd3*) or regulation (*cd2*) displayed a significant reduction in most cutin monomers, including a major decrease in levels of C16-9/10,16-DHFA, as we observed in the *SlDCR*-silenced fruit (Isaacson et al., 2009). Nevertheless, these mutants did not show a major skin injury or signs of surface suberization. It is possible that induction of suberization in tomato fruit, occurring through transcriptional changes, requires a threshold of injury, which takes place in *SlDCR*-silenced fruit. Indeed, the application of petroleum jelly (which served to mimic

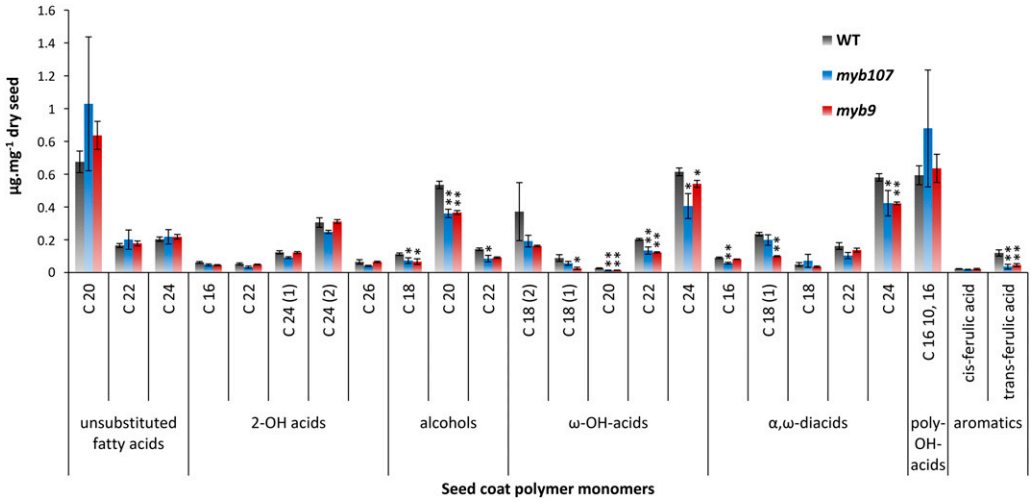

Figure 7. Chemical Analysis of Seed Coat Polymer from *myb9* and *myb107* Mutant Lines.

Chemical analysis via GC-MS of the depolymerized seed coat polymer was performed for mature dry seeds from *myb9* and *myb107* Arabidopsis T-DNA insertion lines. A decrease in aliphatic and aromatic constituents when compared with Col-0 wild type can be observed. Error bars represent SE ($n = 3$; *P value < 0.05, **P value < 0.01, Student's *t* test).

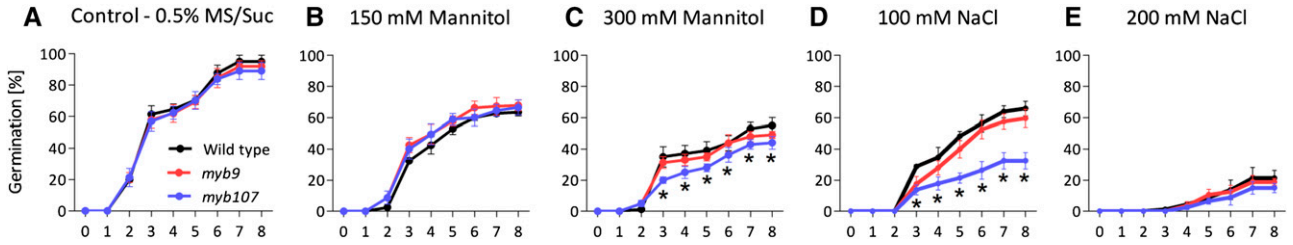

Figure 8. Decreased Germination Rates Were Observed for *myb107* Seeds under Osmotic and Salt Stress.

Germination rates of wild-type (Col-0), *myb9*, and *myb107* mature seeds on control conditions (**[A]**; 0.5% Murashige and Skoog medium/Suc), mild osmotic stress (**[B]**;150 mM mannitol), severe osmotic stress (**[C]**; 300 mM mannitol), mild salt stress (**[D]**; 100 mM NaCl), and severe salt stress (**[E]**; 200 mM NaCl) are shown. Horizontal axis represents days after imbibition. See Supplemental Figure 17 for photographs representing characteristic germination phenotypes under these conditions 8 d after imbibition. Successful germination was scored according to radical emergence (as illustrated in Supplemental Figure 17). Error bars show SE (n = 5, 20 seeds per replicate; *P value < 0.05, Student's t test).

the sealing properties of the cuticle) to developing tomato fruit silenced for *SlDCR* expression and the subsequent arrest of suberin formation, would seem to corroborate this threshold-dependent hypothesis.

In the course of this research, the link between wounding or injury of the cuticle and more specifically cutin deficiency and the resulting formation of suberin was highlighted not only in tomato, but also in apple. Parallel analysis of russeted apples found that the natural coating and suberization of the surface of these fruits was chemically similar to *SlDCR*-silenced tomato fruits. Indeed, the signature metabolites for suberin formation were also identified in the russeted apple surface. These included an increase of ferulates (Serra et al., 2010) and dicarboxylic fatty acids (Kolattukudy, 2001; Compagnon et al., 2009; Yang et al., 2012) and an increase in chain length of the modified FAs (Kolattukudy, 2001; Compagnon et al., 2009). Furthermore, large-scale expression analysis performed in both tomato and apple material confirmed the metabolic shift occurring in the suberized fruit surfaces, corresponding to the reduction in cutin polymer and its replacement with suberin.

Attempts to identify the genetic basis for apple russet thus far pointed to two different underlying genes, both associated with cutin formation. The first, *MdSHN3*, encodes a putative positive transcriptional regulator of cutin deposition (Lashbrooke et al., 2015a) and the other a putative ortholog to an Arabidopsis ABCG transporter protein (AtABCG11) associated with the extracellular secretion of cutin and wax (Panikashvili et al., 2007; Falginella et al., 2015). In both cases, mutations leading to deficiency in the normal deposition of cuticle leads to russet formation. Therefore, it appears that apple has a lower threshold for cuticle failure and subsequent russet (suberin) formation than tomato. The reason for this is unclear, but it may be even more pronounced in other fruit species. Fruit of the closely related pear displays russet even more frequently than apple, while the suberization of netted (or reticulated) melons is considered to be a regular developmental process. It should be noted that abiotic and biotic stresses also cause russet formation, including high levels of surface moisture and humidity, application of chemicals, mechanical wounding and infection, and wounding by pests or microorganisms (Falginella et al., 2015).

Through the widening of the analysis to include additional species from the dicotyledonous Vitaceae, Rosaceae, Brassicaceae, and Solanaceae families, the monocotyledonous Poaceae family, and additional suberin accumulating organs (seeds, tubers, and roots), it was possible to generate a more robust account of gene expression during suberin formation. This multispecies gene expression signature highlighted a number of genes that may be considered fundamental to suberin formation across plant species and provides direction for further studies (Figure 4). The majority of genes have not been associated with suberin formation in the past, though a handful of genes have recently been reported to play a role in this process, thus validating the approach. These include *ABCG6* and *ABCG20*, a pair of homologous transporters shown to contribute to suberin formation in Arabidopsis seed coats (Yadav et al., 2014), as well as the more extensively characterized *CYP86A1*, a cytochrome P450 involved in the synthesis of terminal hydroxy fatty acids with a chain length of <20 carbons (Li et al., 2007; Höfer et al., 2008).

One of the most noteworthy functional groups identified was the one represented by transcriptional regulators including MYB, WRKY, and NAC factors. The MYBs putatively orthologous to AtMYB107 appeared in all seven coexpression analyses and were subject for further characterization. Indeed, phylogenetic and protein motif analysis of the identified MYB factors proposed that in Arabidopsis these proteins are part of a clade of factors containing AtMYB107, AtMYB9, AtMYB93, and AtMYB53. In a previous review, this clade has been described as two separate groups (subgroups 10 and 24; Dubos et al., 2010), but results presented here suggest that this division may be less definitive. Notably, recent work characterizing the diversification of the MYB family in tomato also found subgroups 10 and 24 to be monophyletic (Gates et al., 2016). We defined protein motifs (SUB-I, SUB-II, and SUB-III) in members of both subgroups 10 and 24 that are absent from members of the neighboring subgroups. These motifs were identified in the factors from all six plant species discussed here, namely, SlMYB93, MdMYB53, AtMYB107, AtMYB9, StMYB93, VvMYB107, and OsMYB93, and thus may be used in future studies to identify members of this clade. Furthermore, additional members of this clade from rice and maize (*Zea mays*) have recently been implicated, through coexpression analysis, to be associated with suberin regulation (Wang et al., 2014).

The analysis of *myb107* and *myb9* mutant lines pointed to the involvement of both factors in the developmentally regulated production and deposition of suberin in the seed coat polyester. This polyester, produced in the integument layers of the seed, is

crucial for normal function of the seed, particularly with regard to germination and osmotic stress tolerance. Monomers are thought to predominantly originate from the outer integument layer 1, where suberin-specific gene expression has been previously localized (Beisson et al., 2007). The seed coat polyester plays important roles during seed development, both maintaining dormancy and regulating the transition to germination (Haughn and Chaudhury, 2005; Beisson et al., 2007; Molina et al., 2008). The osmotic sealing of the seed is crucial for these processes, and the production of hydrophobic suberin is the primary mechanism through which this is achieved (Beisson et al., 2007). Chemical analysis confirmed that the seed coat polyester of *myb107* and *myb9* lines was reduced in both aliphatic and aromatic constituents of the suberin polymer. These changes to the seed coat polyester are in agreement with the ones reported in seeds from characterized suberin mutant lines (Beisson et al., 2007; Compagnon et al., 2009). Interestingly, a differential accumulation of other seed coat-associated metabolites, such as waxes, proanthocyanidins, and flavonols, was also observed and may hint at a broader action of AtMYB107 and AtMYB9. The changes to the chemical properties of the mutant seed coats were reflected in several alterations to their structure and morphology, including a reduced mucilage layer observed in both mutant lines, and apparent disorganization of integument layer cells in *myb107* seed coat. Furthermore, seeds from the *myb107* mutant line exhibited lower germination rates when grown under osmotic and salt stresses, a result that is consistent with those previously reported for other suberin mutant seeds, such as *atgpat5*, *atasft*, *atfar1*, *atfar4*, and *atfar5* (Beisson et al., 2007; Gou et al., 2009; Vishwanath et al., 2013). This modulation in germination is likely connected with the sensing of the environment by the seeds and the water potential of the germination media. Apparently the suberin lamella in the seed coat of *myb107* seeds are sufficiently disrupted that normal ion and water channeling is not possible.

The action of these MYB factors is likely exerted through the transcriptional regulation of suberin-associated genes and interaction with each other (Figure 9). Indeed, *AtMYB107* showed a 2-fold upregulation in *myb9* lines, possibly a result of compensation for the downregulation of *AtMYB9*. Promoter binding assays or chromatin immunoprecipitation analysis may be required to fully understand the relationship between these two proteins, but it appears that they may be part of a transcriptional feedback loop as shown previously for other MYB clade members (Frerigmann and Gigolashvili, 2014b, 2014a; Frerigmann et al., 2016). While it is important to note that the known suberin biosynthesis genes *GPAT5*, *ASFT*, and *CYP86A1* were all downregulated in the seed coat of *myb107* and/or *myb9* lines, even more significant was the observed downregulation of a number of the candidates identified through the multispecies coexpression analysis. These include *4CL5*, a gene encoding a 4CL isoenzyme that is somewhat disparate from the other members of this family involved in phenylpropanoid metabolism (Hamberger and Hahlbrock, 2004; Costa et al., 2005). Previous analysis of the lignin content of *4cl5* mutants found no change when compared with the wild type despite the enzyme showing the relevant in vitro activity (Costa et al., 2005). Taken together with the results found here (coexpression with suberin forming tissues and downregulation in *myb107* lines), this suggests that in Arabidopsis seeds, a particular 4CL (namely, 4CL5) may be specific to suberin formation, contributing to the biosynthesis of the aromatic domain. With regards to the extracellular transport of suberin, the identification of the putative lipid transporter, *LTPG5*, being coexpressed with suberin forming tissues, as well as downregulated in *myb107*, is particularly interesting. In previous work, LTPG1 was shown to be active in the extracellular transport of cuticular lipids in Arabidopsis (Debono et al., 2009), while LTPGs have recently been shown to function in the development of both seed coat and pollen apoplastic barriers (Edstam and Edqvist, 2014). It is therefore likely that LTPG5 is involved in suberin deposition in the seed coat of Arabidopsis in a function mediated through MYB107 activity. The most prevalent gene identified in the coexpression analysis (together with the *MYB107* clade) was a *GDSL* esterase, identified in all seven coexpression experiments, suggesting a solid link to suberin formation. In Arabidopsis, this putative *SUS* gene (named here) was found downregulated in both *myb107* and *myb9* lines. Cutin polymerization has recently received significant attention and yet still remains largely undescribed (Domínguez et al., 2015).

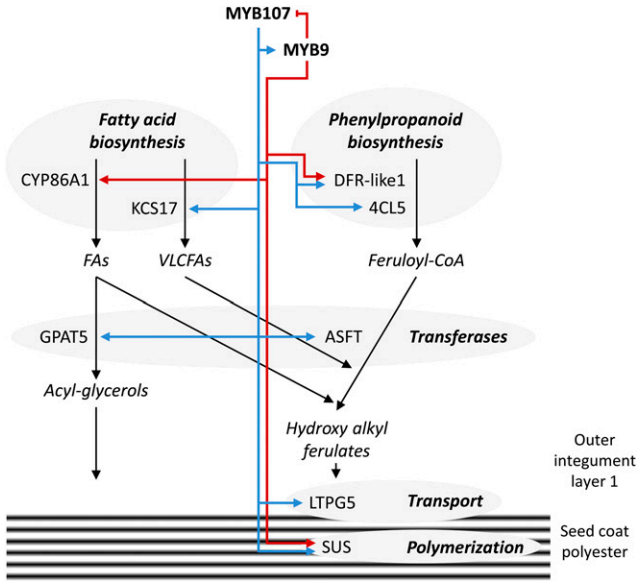

Figure 9. Model for Suberin Formation in the Arabidopsis Seed Coat and the Role of MYB9 and MYB107 Transcription Factors.

MYB9 and MYB107 (represented in bold text) appear to act in tandem to positively regulate various aspects of suberin formation (labeled in bold italics) in the outer integument layer of the seed coat, including fatty acid and phenylpropanoid biosynthesis, and extracellular suberin monomer transport and polymerization. A feedback loop likely exists between MYB9 and MYB107. Proposed downstream targets of MYB107 and MYB9 are shown with blue and red arrows, respectively. The hypothesis is supported by data from the chemical analysis of the seed coat polyester, gene expression data from seeds, as well as seed permeability assays. FA, fatty acid; VLCFAs, very-long-chain fatty acids; GPAT5, GLYCEROL-3-PHOSPHATE ACYLTRANSFERASE5; ASFT, ALIPHATIC SUBERIN FERULOYL TRANSFERASE; KCS17, 3-KETOACYL-COA SYNTHASE17; 4CL5, 4-COUMARATE:COA LIGASE5; DFR-like1, DIHYDROFLAVONOL 4-REDUCTASE-LIKE1; LTPG5, GLYCOSYLPHOSPHATIDYLINOSITOL-ANCHORED LIPID PROTEIN TRANSFER5; SUS, SUBERIN SYNTHASE.

While spontaneous polymerization of cutin monomers was considered, CUS proteins (which have been localized to the extracellular region) have been described to act as acyltransferase enzymes able to link cutin monomers (such as monoglycerols) (Yeats et al., 2012, 2014). In suberin polymer synthesis, SUS proteins may perform an analogous role, making use of monoglycerols and/or hydroxyl-alkyl ferulates as substrates. Indeed, the involvement of putative GDSL orthologs in suberin formation has previously been noted through the identification of candidates in large-scale expression analyses connected with suberin deposition in cork and potato (Soler et al., 2007; Serra et al., 2009).

The broad spectrum of transcriptionally regulated genes together with the metabolic changes effected in knockout lines highlights the multipathway regulatory activity mediated by AtMYB107 and AtMYB9 in the developing Arabidopsis seed coat. It appears that this gene pair coordinates the production of aromatic monomers through the phenylpropanoid pathway, while at the same time activating aliphatic monomer production in fatty acid biosynthesis as well as the extracellular transport and polymerization of these monomers (Figure 9). It is important to note that members of the neighboring clade of MYB transcription factors include (1) AtMYB16 and AtMYB106, both demonstrated previously to regulate cutin formation (Oshima et al., 2013); (2) AtMYB74 and AtMYB102, which have been found to be involved in the plant's response to wounding, salt, and osmotic stresses (Denekamp and Smeekens, 2003; Xu et al., 2015); and (3) AtMYB41, the recently identified stress suberin regulator (Kosma et al., 2014). Together with the classification of AtMYB107 and AtMYB9 as regulators of suberin, this clade appears to include plant surface regulators, with a particular association to osmotic stress. The evolutionary origin of this clade can therefore potentially be linked to the colonization of dry terrestrial environments by early land plants.

METHODS

Plant Material and Transformation

Silencing of *SlDCR* was performed in tomato (*Solanum lycopersicum* cv M82. The SlDCR-RNAi construct was generated by cloning a 378-bp *SlDCR* fragment (from cv M82 cDNA) into pENTR/D-TOPO (Invitrogen). LR Clonase (Invitrogen) was used to recombine this fragment into the pK7GWIWG2(II) binary vector (Karimi et al., 2002). For oligonucleotides, see Supplemental Table 4. Transformation of tomato (cv M82) was performed as previously described (Dan et al., 2006). Two clones of apple (cv Golden Delicious) were analyzed: the normal skinned 'Reinders' and the russeted 'Rugiada'. Three trees for each clone were grown in the experimental orchard of the Fondazione Edmund Mach (Northern Italy) and maintained following standard technical agricultural management for pruning, crop load, and pest-disease control. *Arabidopsis thaliana* plants were grown in a controlled climate room at 20°C, 70% relative humidity, with a 16-h/8-h light/dark cycle. Lines (including Col-0 ecotype and T-DNA insertion lines) were obtained from the ABRC and are listed in Supplemental Table 5. The T-DNA insertion lines were identified using the SIGnAL T-DNA Express Arabidopsis Gene Mapping Tool (http://signal.salk.edu/cgi-bin/tdnaexpress) and screening primers (Supplemental Table 5) designed using the T-DNA Primer Design tool (http://signal.salk.edu/tdnaprimers.2.html) (Alonso et al., 2003).

Sequence Retrieval and Phylogenetic Analysis

Nucleotide and protein sequence retrieval were performed via BLAST analysis. Data were acquired for the various species from the following databases, making use of the gene IDs curated by these databases: SOL Genomics Network database (Fernandez-Pozo et al., 2015), Grape Genome Database (Vitulo et al., 2014), Spud DB (Hirsch et al., 2014), The Arabidopsis Information Resource (Lamesch et al., 2012), Rice Genome Annotation Project (Kawahara et al., 2013), and Genome Database for Rosaceae (Jung et al., 2014). Orthology between species was determined via alignment of relevant protein sequences with the ortholog database from the PLAZA Comparative Genomics Platform (Proost et al., 2015). Gene Ontology enrichment was performed using the PLAZA Comparative Genomics Platform (Proost et al., 2015). Protein alignments were performed using ClustalW (Larkin et al., 2007) and phylogenetic trees visualized using MEGA6 (Tamura et al., 2013). Neighbor-joining trees were constructed with bootstrapping calculated from 1000 instances. Motif discovery was performed for the identified clade of MYB factors using The MEME Suite (Bailey et al., 2009). Identified motifs were screened for presence in neighboring proteins to confirm conservation and then visualized using WebLogo (Crooks et al., 2004).

Light and Electron Microscopy and Histological Sectioning of Seeds

Samples for electron microscopy were fixed and prepared as described previously (Panikashvili et al., 2009). For scanning electron microscopy, samples were analyzed using an XL30 ESEM FEG microscope (FEI) at 5 to 10 kV. Transmission electron microscopy sections (70 nm) were observed with a Technai T12 transmission electron microscope.

For light microscopy, skin tissue samples were fixed and embedded in wax as described previously (Mintz-Oron et al., 2008). Seed sections were performed by collecting whole siliques, which were immediately fixed in 4% paraformaldehyde and 3% glutaraldehyde. The siliques were dehydrated in a graded ethanol series and infiltrated with xylene:paraffin. Sections were cut to 5 to 10 μm on a Leica 2000 microtome and mounted on glass slides. The slides were stained with Sudan IV (Buda et al., 2009) or 0.05% toluidine blue O and then observed with an Olympus CLSM500 microscope.

Chemical Analysis of Cutin and Suberin Polymers and Wax from Fruit Surface and Seed Coat

Fruit skin discs of apple and tomato were prepared for cutin analysis from five fruit per biological sample as previously described (Shi et al., 2013). Isolated cuticles were then washed twice in chloroform for 60 s so as to extract all nonpolymerized extra and intracuticular waxes, before cutin extraction and gas chromatography analysis was performed as described previously (Franke et al., 2005). Extraction and subsequent chemical analysis of the seed coat polyester was performed as described previously (Franke et al., 2005, 2009; Höfer et al., 2008; Compagnon et al., 2009). Waxes were extracted from 100 mg seed samples in 1 mL chloroform for 2 min, before further processing and analysis as described previously (Hen-Avivi et al., 2016). Targeted profiling of aromatic amino acids, soluble proanthocyanidins, and flavonols from mature dry seed samples was performed as described previously (Mizzotti et al., 2014).

Gene Expression Analysis

Nucleic acids were extracted using the CTAB method as described previously (Reid et al., 2006). RT-qPCR analysis was performed for RNA extracted from the mature green stage skin of tomatoes and the mature green stage of seeds from Arabidopsis. The SuperScript VILO cDNA synthesis kit (Invitrogen) was used to synthesize cDNA from DNase-treated total RNA extractions. Analysis was performed using gene-specific oligonucleotides on an ABI 7300 instrument (Applied Biosystems) with the Fast SYBR Green Master Mix (Applied Biosystems) under default parameters. StepOne software (Applied Biosystems) was used to generate expression data. Sequences of gene-specific oligonucleotides are provided in Supplemental Table 4. High-throughput Illumina strand-specific

RNA-seq was performed with RNA extracted from the skin and flesh tissue of five developmental stages of apple for both the 'Reinders' and 'Rugiada' clones (20 samples in total), from mature green stage tomato skin from wild-type and *SlDCR*-RNAi lines in duplicate (four samples in total), and from mature green stage Arabidopsis seeds. Library preparation was performed according to previously described methods (Zhong et al., 2011) and samples run on the Illumina HiSeq 2000 under default parameters generating 50-bp single end reads. Reads were mapped to either the apple (*Malus x domestica*; Jung et al., 2014), tomato (Fernandez-Pozo et al., 2015), or Arabidopsis (Lamesch et al., 2012) predicted transcriptome according to methods described previously (Itkin et al., 2013), generating normalized RPKM values for each gene.

With regards to determining gene expression enrichment in the apple analysis, the fact that at some developmental stages no gene expression was detected in any of the tissues (skin or flesh), and because this phenomenon is not unexpected for cuticle synthesis genes, particularly late in development, as evidenced in Supplemental Figure 9, stages were not considered part of the analysis if there was not at least one tissue with gene expression above zero from that stage. Finally, a proviso that genes must be enriched in at least three stages for a gene to be classified as possessing a russet skin enriched expression pattern was implemented.

Multispecies and Multigene Coexpression Analysis

Genes that are coexpressed with the orthologs to ASFT, GPAT5, and/or CYP86B1 in tomato, apple, grape (*Vitis vinifera*), potato (*Solanum tuberosum*), and Arabidopsis were determined making use of methodologies recently described in detail (Tzfadia et al., 2016). First, large-scale expression data sets for these species were obtained from literature, with the proviso that at least one of the samples analyzed in the data set was a suberin accumulating tissue. To this end, data sets were acquired covering multiple organs and developmental stages for tomato (Tomato Gene Consortium, 2012), potato (Xu et al., 2011), and grape (Fasoli et al., 2012), while a data set analyzing tissue types of developing seeds was acquired for Arabidopsis (Le et al., 2010). The apple data set utilized was generated as part of this work and included skin and flesh tissue of developing apple fruit. Subsequently, orthologs of ASFT, GPAT5, and/or CYP86B1 were identified in each species and used as baits in the coexpression analysis, which made use of a recently described R script (Tzfadia et al., 2016). A list of genes was created for each bait with each gene assigned a Pearson correlation coefficient (*r* value), as an indicator of the level of similarity in expression pattern between the gene and respective bait. Next, a list of coexpressed genes for each species was determined by selecting genes that were coexpressed with multiple baits (i.e., possessing an *r* value above a cutoff dependent on the complexity of the specific data set). A summary of baits used and *r* value cutoffs employed can be seen in Supplemental Table 6. Before comparison of these lists, two further gene lists were retrieved, one from rice genes identified in a large-scale expression analysis to be coexpressed with suberin formation (Shiono et al., 2014), and the second from the genes identified in this study to be upregulated in the fruit skins of *SlDCR*-RNAi tomato lines. Finally, these seven gene lists were compared through the orthology of the respective members of the lists and a coexpression network between the various experiments was visualized using Cytoscape software (Shannon et al., 2003).

Seed Staining Procedures, Suberin Autofluorescence Analysis, and Insulation of Fruit with Petroleum Jelly

For testing the permeability of Arabidopsis seed coats, tetrazolium salt penetration assays were performed (Molina et al., 2008). Seed samples (50 mg each) were incubated in 700 μL 1% aqueous solution of 2,3,5-triphenyltetrazolium chloride at 30°C for 48 h. After incubation, the seeds were washed twice with water and observed under a Nikon SMZ18 stereomicroscope. Images were acquired with a Nikon DS-Ri1 high-resolution camera and qualitatively observed by eye for the degree of redness, indicating movement of the tetrazolium salt into the seed, and staining of the embryonic tissue. Furthermore, an in-house MATLAB script (The MathWorks) was used to quantitatively assess the redness of the individual seeds in each image by quantifying the RGB spectra. Mucilage production properties of mature seeds were analyzed by staining seeds in an aqueous solution of 0.05% ruthenium red for 20 min at room temperature. Following staining the seeds were rinsed in water and imaged via a light microscope. Seed coat suberin autofluorescence analysis was performed as described previously by Beisson et al. (2007). Briefly, mature seeds were epi-illuminated at 365 nm, and autofluorescence was captured at 435 nm by a Zeiss Axiophoto microscope coupled to a digital camera.

To mimic the waterproofing role of the cuticle, fruit of *SlDCR*-RNAi lines (early green stage) were half-covered with petroleum jelly (which was reapplied if required due to growth of the fruit). Fruit at mature green and red ripe stages were harvested, the jelly removed, and fruit photographed.

Germination Assays

For germination assays, freshly harvested seeds were germinated, following imbibition, on 0.5% Murashige and Skoog/sucrose medium supplemented with either 150 mM mannitol, 300 mm Mannitol, 100 mM NaCl, 200 mM NaCl, or not supplemented (control). Twenty seeds from each genotype were grown in separate Petri dishes in five biological replicates, and successful germination was scored according to radical emergence. Germination rates were calculated from 0 to 8 d after imbibition. The experiments were repeated twice, confirming results.

Abscisate Analysis

Hormone extraction was performed as previously described (Kojima et al., 2009; Dobrev and Vankova, 2012; Breitel et al., 2016) with some modifications. Briefly, 10 mg of ground frozen dry seeds were extracted at −20°C with methanol/water/formic acid, containing stable isotope-labeled internal standards. Abscisates were purified by SPE and detected by UPLC-ESI-MS/MS operated in MRM mode. Quantification was done against external calibration curves, using analyte/internal standard peak ratios.

Accession Numbers

Sequence data from this article can be found in the relevant data libraries (TAIR, SGN, GDR, SpudDB, Grape Genome Database, and RGAP) under accession numbers found in Tables 1 and 2 and Supplemental Tables 2 to 5.

Supplemental Data

Supplemental Figure 1. Protein alignment of tomato and Arabidopsis DCR.

Supplemental Figure 2. Organ fusion phenotypes resulting from silencing of *SlDCR* in tomato.

Supplemental Figure 3. Light microscopy of the fruit cuticle of *SlDCR*-RNAi lines.

Supplemental Figure 4. Alignment of tomato and Arabidopsis ASFT proteins.

Supplemental Figure 5. Expression analysis of the *GPAT* gene family in *SlDCR*-silenced tomato plants.

Supplemental Figure 6. Application of petroleum jelly to developing tomato fruit silenced for *SlDCR* expression.

Supplemental Figure 7. Scanning electron microscopy analysis of apple surface.

Supplemental Figure 8. GO enrichment analysis of orthologous genes found upregulated in suberized tomato and apple fruit surfaces.

Supplemental Figure 9. Expression patterns of the coexpression baits and the described MYB factors.

Supplemental Figure 10. Molecular phylogenetic analysis of cutin synthase and putative suberin synthase proteins.

Supplemental Figure 11. Tetrazolium chloride staining assay.

Supplemental Figure 12. Quantification of stain intensity in tetrazolium chloride staining assay.

Supplemental Figure 13. Characterization of *AtMYB107* and *AtMYB9* gene expression in seeds and in the corresponding T-DNA insertion lines.

Supplemental Figure 14. Scanning electron microscopy of Arabidopsis seed coat surface.

Supplemental Figure 15. Seeds of *myb9* and *myb107* mutant lines display higher levels of proanthocyanidins and flavonols and lower levels of wax monomers.

Supplemental Figure 16. Analysis of abscisic acid and its derivatives in *myb107* and *myb9* seeds.

Supplemental Figure 17. Characteristic germination phenotypes under stress conditions.

Supplemental Table 1. Quantification of cuticular waxes from the fruit surface of *SlDCR*-silenced lines.

Supplemental Table 2. Orthologous genes from tomato and apple enriched in both *SlDCR*-RNAi fruit skin and russeted apple skin.

Supplemental Table 3. Multispecies gene expression signature identified for suberin biosynthesis through coexpression analysis.

Supplemental Table 4. Oligonucleotides used in this study for cloning and RT-qPCR analysis.

Supplemental Table 5. Oligonucleotides used in this study for the screening of Arabidopsis T-DNA insertion lines.

Supplemental Table 6. Parameters used for coexpression analysis.

Supplemental Data Set 1. Alignment used to generate the phylogeny shown in Supplemental Figure 5A.

Supplemental Data Set 2. Large-scale RNA-seq expression analysis of skin and flesh tissue of developing apple.

Supplemental Data Set 3. RNA-seq analysis of mature green stage skin tissues of SlDCR-RNAi and wild-type tomato fruit.

Supplemental Data Set 4. Genes identified in the multigene coexpression analysis from tomato, apple, Arabidopsis, potato, and grape.

Supplemental Data Set 5. Alignment used to generate the phylogeny presented in Supplemental Figure 10.

Supplemental Data Set 6. Alignment used to generate the phylogeny presented in Figure 5.

Supplemental Data Set 7. RNA-seq analysis of mature green stage seeds from Arabidopsis (wild type, *myb9*, and *myb107* mutants).

ACKNOWLEDGMENTS

This work was supported by an Israel Science Foundation personal grant to A.A. (ISF Grant 646/11) and by the German Research Society (Deutsche Forschungsgemeinschaft Grant SCH506/12-1 to L.S.). We thank the Adelis Foundation, Leona M. and Harry B. Helmsley Charitable Trust, Jeanne and Joseph Nissim Foundation for Life Sciences, Tom and Sondra Rykoff Family Foundation Research, and the Raymond Burton Plant Genome Research Fund for supporting A.A.'s lab. A.A. is the incumbent of the Peter J. Cohn Professorial Chair. J.L. performed this research as part of a PhD funded by Fondazione Edmund Mach.

AUTHOR CONTRIBUTIONS

J.L. designed and performed research, analyzed data, and was the primary author of the manuscript. H.C. performed experiments, analyzed data, and cowrote the manuscript. D.L.-S., O.T., I.P., and V.Z. performed experiments. H.M., L.T., and L.S. analyzed data. F.C. analyzed data and cowrote the manuscript. A.A. designed research, analyzed data, and cowrote the manuscript. All made relevant contributions to the text and read and approved the final manuscript.

Received June 20, 2016; revised August 24, 2016; accepted September 7, 2016; published September 7, 2016.

REFERENCES

Alonso, J.M., et al. (2003). Genome-wide insertional mutagenesis of *Arabidopsis thaliana*. Science **301:** 653–657.

Bailey, T.L., Boden, M., Buske, F.A., Frith, M., Grant, C.E., Clementi, L., Ren, J., Li, W.W., and Noble, W.S. (2009). MEME SUITE: tools for motif discovery and searching. Nucleic Acids Res. **37:** W202–W208.

Bargel, H., Koch, K., Cerman, Z., and Neinhuis, C. (2006). Structure–function relationships of the plant cuticle and cuticular waxes–a smart material? Funct. Plant Biol. **33:** 893–910.

Beisson, F., Li-Beisson, Y., and Pollard, M. (2012). Solving the puzzles of cutin and suberin polymer biosynthesis. Curr. Opin. Plant Biol. **15:** 329–337.

Beisson, F., Li, Y., Bonaventure, G., Pollard, M., and Ohlrogge, J.B. (2007). The acyltransferase GPAT5 is required for the synthesis of suberin in seed coat and root of Arabidopsis. Plant Cell **19:** 351–368.

Bernards, M.A., and Lewis, N.G. (1992). Alkyl ferulates in wound healing potato tubers. Phytochemistry **31:** 3409–3412.

Breitel, D.A., et al. (2016). AUXIN RESPONSE FACTOR 2 intersects hormonal signals in the regulation of tomato fruit ripening. PLoS Genet. **12:** e1005903.

Buda, G.J., Isaacson, T., Matas, A.J., Paolillo, D.J., and Rose, J.K. (2009). Three-dimensional imaging of plant cuticle architecture using confocal scanning laser microscopy. Plant J. **60:** 378–385.

Chen, G., Komatsuda, T., Ma, J.F., Li, C., Yamaji, N., and Nevo, E. (2011a). A functional cutin matrix is required for plant protection against water loss. Plant Signal. Behav. **6:** 1297–1299.

Chen, X., Truksa, M., Snyder, C.L., El-Mezawy, A., Shah, S., and Weselake, R.J. (2011b). Three homologous genes encoding sn-glycerol-3-phosphate acyltransferase 4 exhibit different expression patterns and functional divergence in *Brassica napus*. Plant Physiol. **155:** 851–865.

Cominelli, E., Sala, T., Calvi, D., Gusmaroli, G., and Tonelli, C. (2008). Over-expression of the Arabidopsis AtMYB41 gene alters cell expansion and leaf surface permeability. Plant J. **53:** 53–64.

Compagnon, V., Diehl, P., Benveniste, I., Meyer, D., Schaller, H., Schreiber, L., Franke, R., and Pinot, F. (2009). CYP86B1 is required for very long chain omega-hydroxyacid and alpha, omega -dicarboxylic acid synthesis in root and seed suberin polyester. Plant Physiol. **150:** 1831–1843.

Costa, M.A., et al. (2005). Characterization in vitro and in vivo of the putative multigene 4-coumarate:CoA ligase network in Arabidopsis: syringyl lignin and sinapate/sinapyl alcohol derivative formation. Phytochemistry **66:** 2072–2091.

Crooks, G.E., Hon, G., Chandonia, J.M., and Brenner, S.E. (2004). WebLogo: a sequence logo generator. Genome Res. **14:** 1188–1190.

Dan, Y., Yan, H., Munyikwa, T., Dong, J., Zhang, Y., and Armstrong, C.L. (2006). MicroTom–a high-throughput model transformation system for functional genomics. Plant Cell Rep. **25:** 432–441.

Dean, B.B., and Kolattukudy, P.E. (1976). Synthesis of suberin during wound-healing in jade leaves, tomato fruit, and bean pods. Plant Physiol. **58:** 411–416.

Debono, A., Yeats, T.H., Rose, J.K., Bird, D., Jetter, R., Kunst, L., and Samuels, L. (2009). Arabidopsis LTPG is a glycosylphosphatidylinositol-anchored lipid transfer protein required for export of lipids to the plant surface. Plant Cell **21:** 1230–1238.

Denekamp, M., and Smeekens, S.C. (2003). Integration of wounding and osmotic stress signals determines the expression of the AtMYB102 transcription factor gene. Plant Physiol. **132:** 1415–1423.

Dobrev, P.I., and Vankova, R. (2012). Quantification of abscisic acid, cytokinin, and auxin content in salt-stressed plant tissues. Methods Mol. Biol. **913:** 251–261.

Domergue, F., Vishwanath, S.J., Joubès, J., Ono, J., Lee, J.A., Bourdon, M., Alhattab, R., Lowe, C., Pascal, S., Lessire, R., and Rowland, O. (2010). Three Arabidopsis fatty acyl-coenzyme A reductases, FAR1, FAR4, and FAR5, generate primary fatty alcohols associated with suberin deposition. Plant Physiol. **153:** 1539–1554.

Domínguez, E., Heredia-Guerrero, J.A., and Heredia, A. (2015). Plant cutin genesis: unanswered questions. Trends Plant Sci. **20:** 551–558.

Dubos, C., Stracke, R., Grotewold, E., Weisshaar, B., Martin, C., and Lepiniec, L. (2010). MYB transcription factors in Arabidopsis. Trends Plant Sci. **15:** 573–581.

Edstam, M.M., and Edqvist, J. (2014). Involvement of GPI-anchored lipid transfer proteins in the development of seed coats and pollen in *Arabidopsis thaliana*. Physiol. Plant. **152:** 32–42.

Ebizuka, Y., Katsube, Y., Tsutsumi, T., Kushiro, T., and Shibuya, M. (2003). Functional genomics approach to the study of triterpene biosynthesis. Pure Appl. Chem. **75:** 369–374.

Falginella, L., Cipriani, G., Monte, C., Gregori, R., Testolin, R., Velasco, R., Troggio, M., and Tartarini, S. (2015). A major QTL controlling apple skin russeting maps on the linkage group 12 of 'Renetta Grigia di Torriana'. BMC Plant Biol. **15:** 150.

Fasoli, M., et al. (2012). The grapevine expression atlas reveals a deep transcriptome shift driving the entire plant into a maturation program. Plant Cell **24:** 3489–3505.

Fernandez-Pozo, N., Menda, N., Edwards, J.D., Saha, S., Tecle, I.Y., Strickler, S.R., Bombarely, A., Fisher-York, T., Pujar, A., Foerster, H., Yan, A., and Mueller, L.A. (2015). The Sol Genomics Network (SGN): from genotype to phenotype to breeding. Nucleic Acids Res. **43:** D1036–D1041.

Franke, R., Briesen, I., Wojciechowski, T., Faust, A., Yephremov, A., Nawrath, C., and Schreiber, L. (2005). Apoplastic polyesters in Arabidopsis surface tissues: a typical suberin and a particular cutin. Phytochemistry **66:** 2643–2658.

Franke, R., Höfer, R., Briesen, I., Emsermann, M., Efremova, N., Yephremov, A., and Schreiber, L. (2009). The DAISY gene from Arabidopsis encodes a fatty acid elongase condensing enzyme involved in the biosynthesis of aliphatic suberin in roots and the chalaza-micropyle region of seeds. Plant J. **57:** 80–95.

Frerigmann, H., and Gigolashvili, T. (2014a). Update on the role of R2R3-MYBs in the regulation of glucosinolates upon sulfur deficiency. Front. Plant Sci. **5:** 626.

Frerigmann, H., and Gigolashvili, T. (2014b). MYB34, MYB51, and MYB122 distinctly regulate indolic glucosinolate biosynthesis in *Arabidopsis thaliana*. Mol. Plant **7:** 814–828.

Frerigmann, H., Piślewska-Bednarek, M., Sánchez-Vallet, A., Molina, A., Glawischnig, E., Gigolashvili, T., and Bednarek, P. (2016). Regulation of pathogen-triggered tryptophan metabolism in *Arabidopsis thaliana* by MYB transcription factors and indole glucosinolate conversion products. Mol. Plant **9:** 682–695.

Gates, D.J., Strickler, S.R., Mueller, L.A., Olson, B.J., and Smith, S.D. (2016). Diversification of R2R3-MYB transcription factors in the tomato family Solanaceae. J. Mol. Evol. **83:** 26–37.

Gou, J.Y., Yu, X.H., and Liu, C.J. (2009). A hydroxycinnamoyltransferase responsible for synthesizing suberin aromatics in Arabidopsis. Proc. Natl. Acad. Sci. USA **106:** 18855–18860.

Hamberger, B., and Hahlbrock, K. (2004). The 4-coumarate:CoA ligase gene family in *Arabidopsis thaliana* comprises one rare, sinapate-activating and three commonly occurring isoenzymes. Proc. Natl. Acad. Sci. USA **101:** 2209–2214.

Haughn, G., and Chaudhury, A. (2005). Genetic analysis of seed coat development in Arabidopsis. Trends Plant Sci. **10:** 472–477.

Hen-Avivi, S., et al. (2016). A metabolic gene cluster in the wheat W1 and the barley Cer-cqu loci determines β-diketone biosynthesis and glaucousness. Plant Cell **28:** 1440–1460.

Heredia, A. (2003). Biophysical and biochemical characteristics of cutin, a plant barrier biopolymer. Biochim. Biophys. Acta **1620:** 1–7.

Hirsch, C.D., Hamilton, J.P., Childs, K.L., Cepela, J., Crisovan, E., Vaillancourt, B., Hirsch, C.N., Habermann, M., Neal, B., and Buell, C.R. (2014). Spud DB: A resource for mining sequences, genotypes, and phenotypes to accelerate potato breeding. Plant Genome **7:** 1–12.

Höfer, R., Briesen, I., Beck, M., Pinot, F., Schreiber, L., and Franke, R. (2008). The Arabidopsis cytochrome P450 CYP86A1 encodes a fatty acid omega-hydroxylase involved in suberin monomer biosynthesis. J. Exp. Bot. **59:** 2347–2360.

Isaacson, T., Kosma, D.K., Matas, A.J., Buda, G.J., He, Y., Yu, B., Pravitasari, A., Batteas, J.D., Stark, R.E., Jenks, M.A., and Rose, J.K. (2009). Cutin deficiency in the tomato fruit cuticle consistently affects resistance to microbial infection and biomechanical properties, but not transpirational water loss. Plant J. **60:** 363–377.

Itkin, M., et al. (2013). Biosynthesis of antinutritional alkaloids in solanaceous crops is mediated by clustered genes. Science **341:** 175–179.

Jung, S., et al. (2014). The Genome Database for Rosaceae (GDR): year 10 update. Nucleic Acids Res. **42:** D1237–D1244.

Karimi, M., Inzé, D., and Depicker, A. (2002). GATEWAY vectors for Agrobacterium-mediated plant transformation. Trends Plant Sci. **7:** 193–195.

Kawahara, Y., et al. (2013). Improvement of the Oryza sativa Nipponbare reference genome using next generation sequence and optical map data. Rice (NY) **6:** 4.

Khanal, B.P., Grimm, E., and Knoche, M. (2013). Russeting in apple and pear: a plastic periderm replaces a stiff cuticle. AoB Plants **5:** pls048.

Kojima, M., Kamada-Nobusada, T., Komatsu, H., Takei, K., Kuroha, T., Mizutani, M., Ashikari, M., Ueguchi-Tanaka, M., Matsuoka, M., Suzuki, K., and Sakakibara, H. (2009). Highly sensitive and high-throughput analysis of plant hormones using MS-probe modification and liquid chromatography-tandem mass spectrometry: an application for hormone profiling in *Oryza sativa*. Plant Cell Physiol. **50:** 1201–1214.

Kolattukudy, P.E. (2001). Polyesters in higher plants. Adv. Biochem. Eng. Biotechnol. **71:** 1–49.

Kosma, D.K., Murmu, J., Razeq, F.M., Santos, P., Bourgault, R., Molina, I., and Rowland, O. (2014). AtMYB41 activates ectopic suberin synthesis and assembly in multiple plant species and cell types. Plant J. **80:** 216–229.

Lallemand, B., Erhardt, M., Heitz, T., and Legrand, M. (2013). Sporopollenin biosynthetic enzymes interact and constitute a metabolon localized to the endoplasmic reticulum of tapetum cells. Plant Physiol. **162:** 616–625.

Lamesch, P., et al. (2012). The Arabidopsis Information Resource (TAIR): improved gene annotation and new tools. Nucleic Acids Res. **40:** D1202–D1210.

Larkin, M.A., et al. (2007). Clustal W and Clustal X version 2.0. Bioinformatics **23:** 2947–2948.

Lashbrooke, J., Aharoni, A., and Costa, F. (2015a). Genome investigation suggests MdSHN3, an APETALA2-domain transcription factor gene, to be a positive regulator of apple fruit cuticle formation and an inhibitor of russet development. J. Exp. Bot. **66:** 6579–6589.

Lashbrooke, J., et al. (2015b). The tomato MIXTA-like transcription factor coordinates fruit epidermis conical cell development and cuticular lipid biosynthesis and assembly. Plant Physiol. **169:** 2553–2571.

Le, B.H., et al. (2010). Global analysis of gene activity during Arabidopsis seed development and identification of seed-specific transcription factors. Proc. Natl. Acad. Sci. USA **107:** 8063–8070.

Lee, S.B., Jung, S.J., Go, Y.S., Kim, H.U., Kim, J.K., Cho, H.J., Park, O.K., and Suh, M.C. (2009). Two Arabidopsis 3-ketoacyl CoA synthase genes, KCS20 and KCS2/DAISY, are functionally redundant in cuticular wax and root suberin biosynthesis, but differentially controlled by osmotic stress. Plant J. **60:** 462–475.

Li, Y., Beisson, F., Koo, A.J., Molina, I., Pollard, M., and Ohlrogge, J. (2007). Identification of acyltransferases required for cutin biosynthesis and production of cutin with suberin-like monomers. Proc. Natl. Acad. Sci. USA **104:** 18339–18344.

Li-Beisson, Y., et al. (2013). Acyl-lipid metabolism. Arabidopsis Book **11:** e0161.

Lippold, F., Sanchez, D.H., Musialak, M., Schlereth, A., Scheible, W.R., Hincha, D.K., and Udvardi, M.K. (2009). AtMyb41 regulates transcriptional and metabolic responses to osmotic stress in Arabidopsis. Plant Physiol. **149:** 1761–1772.

Mintz-Oron, S., Mandel, T., Rogachev, I., Feldberg, L., Lotan, O., Yativ, M., Wang, Z., Jetter, R., Venger, I., Adato, A., and Aharoni, A. (2008). Gene expression and metabolism in tomato fruit surface tissues. Plant Physiol. **147:** 823–851.

Mizzotti, C., Ezquer, I., Paolo, D., Rueda-Romero, P., Guerra, R.F., Battaglia, R., Rogachev, I., Aharoni, A., Kater, M.M., Caporali, E., and Colombo, L. (2014). SEEDSTICK is a master regulator of development and metabolism in the Arabidopsis seed coat. PLoS Genet. **10:** e1004856.

Mochizuki, S., Sugimoto, K., Koeduka, T., and Matsui, K. (2016). Arabidopsis lipoxygenase 2 is essential for formation of green leaf volatiles and five-carbon volatiles. FEBS Lett. **590:** 1017–1027.

Molina, I., Li-Beisson, Y., Beisson, F., Ohlrogge, J.B., and Pollard, M. (2009). Identification of an Arabidopsis feruloyl-coenzyme A transferase required for suberin synthesis. Plant Physiol. **151:** 1317–1328.

Molina, I., Ohlrogge, J.B., and Pollard, M. (2008). Deposition and localization of lipid polyester in developing seeds of *Brassica napus* and *Arabidopsis thaliana*. Plant J. **53:** 437–449.

Oshima, Y., Shikata, M., Koyama, T., Ohtsubo, N., Mitsuda, N., and Ohme-Takagi, M. (2013). MIXTA-like transcription factors and WAX INDUCER1/SHINE1 coordinately regulate cuticle development in Arabidopsis and *Torenia fournieri*. Plant Cell **25:** 1609–1624.

Panikashvili, D., Shi, J.X., Schreiber, L., and Aharoni, A. (2009). The Arabidopsis DCR encoding a soluble BAHD acyltransferase is required for cutin polyester formation and seed hydration properties. Plant Physiol. **151:** 1773–1789.

Panikashvili, D., Savaldi-Goldstein, S., Mandel, T., Yifhar, T., Franke, R.B., Höfer, R., Schreiber, L., Chory, J., and Aharoni, A. (2007). The Arabidopsis DESPERADO/AtWBC11 transporter is required for cutin and wax secretion. Plant Physiol. **145:** 1345–1360.

Peschel, S., Franke, R., Schreiber, L., and Knoche, M. (2007). Composition of the cuticle of developing sweet cherry fruit. Phytochemistry **68:** 1017–1025.

Petit, J., Bres, C., Mauxion, J.P., Tai, F.W., Martin, L.B., Fich, E.A., Joubés, J., Rose, J.K., Domergue, F., and Rothan, C. (2016). The gycerol-3-phosphate acyltransferase GPAT6 from tomato plays a central role in fruit cutin biosynthesis. Plant Physiol. **171:** 894–913.

Pollard, M., Beisson, F., Li, Y., and Ohlrogge, J.B. (2008). Building lipid barriers: biosynthesis of cutin and suberin. Trends Plant Sci. **13:** 236–246.

Proost, S., Van Bel, M., Vaneechoutte, D., Van de Peer, Y., Inzé, D., Mueller-Roeber, B., and Vandepoele, K. (2015). PLAZA 3.0: an access point for plant comparative genomics. Nucleic Acids Res. **43:** D974–D981.

Rashid, A., and Deyholos, M.K. (2011). PELPK1 (At5g09530) contains a unique pentapeptide repeat and is a positive regulator of germination in *Arabidopsis thaliana*. Plant Cell Rep. **30:** 1735–1745.

Reid, K.E., Olsson, N., Schlosser, J., Peng, F., and Lund, S.T. (2006). An optimized grapevine RNA isolation procedure and statistical determination of reference genes for real-time RT-PCR during berry development. BMC Plant Biol. **6:** 27.

Roppolo, D., Boeckmann, B., Pfister, A., Boutet, E., Rubio, M.C., Dénervaud-Tendon, V., Vermeer, J.E., Gheyselinck, J., Xenarios, I., and Geldner, N. (2014). Functional and evolutionary analysis of the CASPARIAN STRIP MEMBRANE DOMAIN PROTEIN family. Plant Physiol. **165:** 1709–1722.

Schreiber, L. (2010). Transport barriers made of cutin, suberin and associated waxes. Trends Plant Sci. **15:** 546–553.

Schreiber, L., Franke, R., and Hartmann, K. (2005). Wax and suberin development of native and wound periderm of potato (*Solanum tuberosum* L.) and its relation to peridermal transpiration. Planta **220:** 520–530.

Schuetz, M., Benske, A., Smith, R.A., Watanabe, Y., Tobimatsu, Y., Ralph, J., Demura, T., Ellis, B., and Samuels, A.L. (2014). Laccases direct lignification in the discrete secondary cell wall domains of protoxylem. Plant Physiol. **166:** 798–807.

Serra, O., Figueras, M., Franke, R., Prat, S., and Molinas, M. (2010). Unraveling ferulate role in suberin and periderm biology by reverse genetics. Plant Signal. Behav. **5:** 953–958.

Serra, O., Soler, M., Hohn, C., Sauveplane, V., Pinot, F., Franke, R., Schreiber, L., Prat, S., Molinas, M., and Figueras, M. (2009). CYP86A33-targeted gene silencing in potato tuber alters suberin composition, distorts suberin lamellae, and impairs the periderm's water barrier function. Plant Physiol. **149:** 1050–1060.

Shannon, P., Markiel, A., Ozier, O., Baliga, N.S., Wang, J.T., Ramage, D., Amin, N., Schwikowski, B., and Ideker, T. (2003). Cytoscape: a software environment for integrated models of biomolecular interaction networks. Genome Res. **13:** 2498–2504.

Shi, J.X., et al. (2013). The tomato SlSHINE3 transcription factor regulates fruit cuticle formation and epidermal patterning. New Phytol. **197:** 468–480.

Shi, J.X., Malitsky, S., De Oliveira, S., Branigan, C., Franke, R.B., Schreiber, L., and Aharoni, A. (2011). SHINE transcription factors act redundantly to pattern the archetypal surface of Arabidopsis flower organs. PLoS Genet. **7:** e1001388.

Shiono, K., Yamauchi, T., Yamazaki, S., Mohanty, B., Malik, A.I., Nagamura, Y., Nishizawa, N.K., Tsutsumi, N., Colmer, T.D., and Nakazono, M. (2014). Microarray analysis of laser-microdissected tissues indicates the biosynthesis of suberin in the outer part of roots during formation of a barrier to radial oxygen loss in rice (*Oryza sativa*). J. Exp. Bot. **65:** 4795–4806.

Soler, M., Serra, O., Molinas, M., Huguet, G., Fluch, S., and Figueras, M. (2007). A genomic approach to suberin biosynthesis and cork differentiation. Plant Physiol. **144:** 419–431.

Tamura, K., Stecher, G., Peterson, D., Filipski, A., and Kumar, S. (2013). MEGA6: Molecular Evolutionary Genetics Analysis version 6.0. Mol. Biol. Evol. **30:** 2725–2729.

Tomato Gene Consortium (2012). The tomato genome sequence provides insights into fleshy fruit evolution. Nature **485:** 635–641.

Tzfadia, O., Diels, T., De Meyer, S., Vandepoele, K., Aharoni, A., and Van de Peer, Y. (2016). CoExpNetViz: Comparative Co-Expression Networks Construction and Visualization Tool. Front. Plant Sci. **6:** 1194.

Vishwanath, S.J., Kosma, D.K., Pulsifer, I.P., Scandola, S., Pascal, S., Joubès, J., Dittrich-Domergue, F., Lessire, R., Rowland, O., and Domergue, F. (2013). Suberin-associated fatty alcohols in Arabidopsis: distributions in roots and contributions to seed coat barrier properties. Plant Physiol. **163:** 1118–1132.

Vitulo, N., Forcato, C., Carpinelli, E.C., Telatin, A., Campagna, D., D'Angelo, M., Zimbello, R., Corso, M., Vannozzi, A., Bonghi, C.,

Lucchin, M., and Valle, G. (2014). A deep survey of alternative splicing in grape reveals changes in the splicing machinery related to tissue, stress condition and genotype. BMC Plant Biol. **14:** 99.

Wang, L., et al. (2014). Comparative analyses of C_4 and C_3 photosynthesis in developing leaves of maize and rice. Nat. Biotechnol. **32:** 1158–1165.

Welinder, K.G., Justesen, A.F., Kjaersgård, I.V., Jensen, R.B., Rasmussen, S.K., Jespersen, H.M., and Duroux, L. (2002). Structural diversity and transcription of class III peroxidases from *Arabidopsis thaliana*. Eur. J. Biochem. **269:** 6063–6081.

Xu, R., Wang, Y., Zheng, H., Lu, W., Wu, C., Huang, J., Yan, K., Yang, G., and Zheng, C. (2015). Salt-induced transcription factor MYB74 is regulated by the RNA-directed DNA methylation pathway in Arabidopsis. J. Exp. Bot. **66:** 5997–6008.

Xu, X., et al.; Potato Genome Sequencing Consortium (2011) Genome sequence and analysis of the tuber crop potato. Nature **475:** 189–195.

Yadav, V., Molina, I., Ranathunge, K., Castillo, I.Q., Rothstein, S.J., and Reed, J.W. (2014). ABCG transporters are required for suberin and pollen wall extracellular barriers in Arabidopsis. Plant Cell **26:** 3569–3588.

Yang, T.J., Perry, P.J., Ciani, S., Pandian, S., and Schmidt, W. (2008). Manganese deficiency alters the patterning and development of root hairs in Arabidopsis. J. Exp. Bot. **59:** 3453–3464.

Yang, W., Pollard, M., Li-Beisson, Y., Beisson, F., Feig, M., and Ohlrogge, J. (2010). A distinct type of glycerol-3-phosphate acyltransferase with sn-2 preference and phosphatase activity producing 2-monoacylglycerol. Proc. Natl. Acad. Sci. USA **107:** 12040–12045.

Yang, W., Simpson, J.P., Li-Beisson, Y., Beisson, F., Pollard, M., and Ohlrogge, J.B. (2012). A land-plant-specific glycerol-3-phosphate acyltransferase family in Arabidopsis: substrate specificity, sn-2 preference, and evolution. Plant Physiol. **160:** 638–652.

Yeats, T.H., Martin, L.B., Viart, H.M., Isaacson, T., He, Y., Zhao, L., Matas, A.J., Buda, G.J., Domozych, D.S., Clausen, M.H., and Rose, J.K. (2012). The identification of cutin synthase: formation of the plant polyester cutin. Nat. Chem. Biol. **8:** 609–611.

Yeats, T.H., Huang, W., Chatterjee, S., Viart, H.M., Clausen, M.H., Stark, R.E., and Rose, J.K. (2014). Tomato Cutin Deficient 1 (CD1) and putative orthologs comprise an ancient family of cutin synthase-like (CUS) proteins that are conserved among land plants. Plant J. **77:** 667–675.

Zhao, Q., Nakashima, J., Chen, F., Yin, Y., Fu, C., Yun, J., Shao, H., Wang, X., Wang, Z.Y., and Dixon, R.A. (2013). Laccase is necessary and nonredundant with peroxidase for lignin polymerization during vascular development in Arabidopsis. Plant Cell **25:** 3976–3987.

Zhong, S., Joung, J.G., Zheng, Y., Chen, Y.R., Liu, B., Shao, Y., Xiang, J.Z., Fei, Z., and Giovannoni, J.J. (2011). High-throughput illumina strand-specific RNA sequencing library preparation. Cold Spring Harb. Protoc. **2011:** 940–949.